Development of Equipment and Techniques to Evaluate Boundary Effects of Methane/Coal Dust Explosion

Final Report

by

John H.S. Lee, R. Knystautas, N. Craft, F. Band and P.Y. Kang

Department of Mechanical Engineering, McGill University

Work on this project was conducted under the auspices of the Canada Centre for Mineral and Energy Technology, Energy, Mines and Resources, Canada.

DSS FILE NUMBER : 23SV 23440-2-9078

DSS CONTRACT SERIAL NUMBER : OSV82-00039

CANMET PROJECT NUMBER : 430402

CANMET SCIENTIFIC AUTHORITY : Dr. K.K. Feng

DATE: March 1984

This report should be cited as Contract Report No: OSV82-00039

74 pp

JUL 30 1984

MICROMEDIA

I. GENERAL REMARKS

Many mine accidents occur when a large methane-air zone formed near the face that is being mined is accidentally ignited. The rapidly expanding gases generated by this primary blast produce a flow field ahead of the propagating flame. This flow field will then entrain coal dust layered on the floor and on rafters forming an explosive mixture into which the flame will propagate. Turbulence is generated when the flow passes over equipment and structures that are in the mine which further enhances the burning rate. In this way the explosion may rip through the entire gallery, constantly generating an explosive dust air mixture ahead of itself. It is easy to visualize that in this scenario the flame will encounter the whole gamut of fuel-air-inertant mixtures including; a) pure gas explosions, b) gas explosions with both combustible and inert dusts, c) dust explosions with non-flammable mixtures of methane gas, and d) pure dust explosions, as well as a wide range of turbulent intensities.

The explosibility of various dusts was first investigated by Hartmann,[1] who put emphasis on classifying dusts by such criteria as minimum explosive concentration, minimum auto-ignition temperature, etc., in order to guide the design of safety measures for the safe handling of each dust. Hartmann's experiments were refined and expanded on by Barthnecht,[2] Field[3] and Swift,[4] among others to the point that a considerable body of engineering data exists today. In more recent years, some experiments were performed with the goal of acquiring more fundamental knowledge of the parameters and mechanisms which control the reaction rates, the extent of the burning and other phenomena on the basic physical and chemical level. Kaufman,[5] and Wolanski[6] have been particularly active in this area, studying the initiation of dust explosions by various electrical, chemical and physical means, studying details of dust dispersions, laminar

dust flames in zero-gravity environment, dust-gaseous fuel mixtures and even dust detonations.

Most research however, is limited to bench scale experiments and it remains a fundamental problem to scale these results to that of a real explosion. As well, the effect of changing the geometry of the enclosure (eg., the L/D ratio of the mine gallery, etc.) is not well understood. In this regard, we have performed experiments up to 1 m scale to complement the small scale results currently produced at EMR. These results will also be used to develop scaling laws to guide in the development of a large scale testing program to be carried out at EMR in conjunction with McGill.

A critical parameter affecting the degree of physical and structural damage from a dust explosion is the turbulence of the flow field into which the explosion propagates. To study this effect experimentally, a spherical bomb has been built in which the degree of turbulence of the cold dust-air mixture can be varied. Preliminary experiments performed in this sphere indicate that the rate of combustion of the dust air mixture can be increased by as much as 300% by making the combustion environment sufficiently turbulent.

A program has been developed whereby the properties of hybrid explosions are studied in a systematic manner. A medium scale apparatus (156 liters) was developed to study the propagation of the explosion and the pressure development. It has been shown that small amounts of methane gas, below the lower explosive limit, can sensitize even a rich dust-air mixture. The explosion pressure does not vary significantly, but the rate of pressure rise increases markedly. Also, it has been shown that dust, both inert and combustible, can inhibit a stoichiometric methane-air

explosion. Again, the explosion pressure is only slightly reduced, whereas the rate of pressure rise in the vessel is retarded to a significant extent.

Since the acceleration of dust flames by obstacles in a mine gallery is a determining factor as to whether the explosion is transmitted to other parts of the mine or is extinguished, an apparatus has been built to study flame acceleration by repeated obstacles in a long circular tube. That such acceleration occurs and is of high magnitude was shown by preliminary experiments. Problems associated with obtaining a uniform dust dispersion in a long tube were identified and a system has been developed to overcome these.

II. TURBULENT COMBUSTION OF DUST AND METHANE

A. Turbulent Dust Combustion

It has long been known that turbulence increases the rate of burning of gaseous fuels and liquid droplets. This phenomenon can generally be attributed to the increase in the area of the flame front due to wrinkling by eddies whose length is of the order of the flame thickness, and to increase in the energy transport coefficient attributed to microscale turbulence.

Because of the obvious similarity between liquid droplet combustion and dust combustion, it must be presumed that dusts would behave in a similar manner with respect to turbulence. However, little has been done so far to assess this phenomenon experimentally in explosions.

Previous studies[7,8] have found that initial turbulence increases the maximum rate of pressure rise, but leaves the maximum pressure developed relatively unaffected. All of these studies, however, were conducted in vessels which had previously been evacuated and where turbulence was created by the dispersing air jet alone. In some cases, the dispersion air pressure was taken as a measure of the induced turbulence,[2] while in others, turbulence was quantified by the delay between dispersion of the dust and ignition of the mixture.[1] Both these methods have the disadvantage of being unsteady. The novelty of our experiment lies in the fact that the turbulence is much better controlled and can be varied independently of the dispersion mechanism itself.

Apparatus

The apparatus (Fig. 1) consists of a 333 liter spherical vessel (diameter = 0.9 m). Variable amounts of dust were placed in a dust cup located at the bottom of the sphere. The dust was dispersed by discharging a 1.5 liter vessel directly onto it by the activation of a solenoid valve. An igniter using exploding brass wire of 0.003 inch diameter was positioned in the center of the sphere. The delay between dispersion (activation of the solenoid valve) and ignition was controlled by means of a calibrated timer to a precision of plus or minus 10 ms.

Turbulence was induced inside the sphere by injecting air at a steady rate through a circular ring (diameter = 43 cm) made of half-inch copper tubing in which ten holes of 1 mm diameter were drilled. The holes were distributed evenly on the circumference of the ring and a uniform flow direction, perpendicular to the vertical axis of the sphere was achieved by orienting the five holes in one hemisphere in a given direction, while the five holes in the other hemisphere were facing the opposite direction. The

level of turbulence was controlled by a pressure regulator upstream of the turbulence ring. The flow being choked at the turbulence ring, the increase in pressure inside the vessel due to air inflow did not vary the mass rate of air flow. This rate was taken as a measure of the initial turbulence level. To ensure that ignition occurred at atmospheric pressure, the sphere had to be partially evacuated prior to injecting the turbulence air. This was done by means of a vacuum pump. The instrumentation consisted in a PCB piezoelectric pressure transducer coupled to an oscilloscope. A permanent record of each run was obtained by taking a Polaroid picture of the oscilloscope trace (Fig. 2).

Experimental Procedure

To establish some confidence in the ability of the apparatus to produce repeatable and trustworthy results, the effect of varying dust concentration and ignition timing delay was first measured. In this set of experiments, the turbulence mechanism was not in use: the dust cup was put inside the sphere, the dispersion air was discharged onto the dust, and after predetermined delay, the mixture was ignited.

For the main set of experiments concerning turbulent explosions, the vessel was first evacuated to a specific pressure. The pressure regulator was then set to obtain a known rate of air flow through the turbulent ring. When the pressure inside the vessel reached one atmosphere, the solenoid valve was opened to disperse the dust and, after a predetermined delay, the dust was ignited.

DISCUSSION OF THE RESULTS:

Effect of Dust Concentration

The effect of dust concentration on the maximum pressure developed and maximum rate of pressure rise are shown in Figures 2 and 3. The lower explosive concentration is seen to be in the vicinity of 100 gms/m^3. Our experiments have failed to establish an upper explosive concentration as it is seen that the peak pressure and maximum rate of pressure rise reaches a constant value past 600 gms/m^3. This result is in agreement with the work of Hertzberg[10] on coal dust and can be attributed to the inability of the extraneous dust to absorb heat quickly enough to slow down and quench the reactions. Our results are in good agreement with those of Hartmann[1] as the figure shows. At sufficiently high concentrations, the observed peak pressure was only slightly lower than the value of 980 kPa calculated for the constant volume, adiabatic combustion of cornstarch at the stoichiometric concentration of 270 grams/cu meters based on the approximate formula $C_6H_{10}O_5$ for cornstarch.[11] Maximum overpressure is limited by the amount of oxidizer inside the vessel, and cannot increase past the point where all the oxidizer is consumed.

Effect of Ignition Timing Delay

The dust is dispersed by discharging a high pressure reservoir directly onto the cup. Due to the very high Reynolds number of the jet, the dispersion produces an important amount of turbulence. A time-history of the situation prevailing inside the sphere from the instant of dispersion may be described qualitatively as follows: the jet first lifts the dust from the cup and disperses it into the sphere. Due to asymmetries in the impact of the jet and the dust particles, the dust concentration inside the sphere is not homogeneous at first. After the dust has been entirely lifted

from the cup, the jet keeps swirling the mixture, making the concentration more homogeneous, and the flow field more turbulent. Then, after the bottle has been emptied, viscous dissipation diffuses the turbulence and gravity acts on the particles, causing them to fall out of suspension.

According to this description, we must expect that a very short ignition timing delay will produce a weak explosion since large concentration gradients are not favorable to quick propagation, and that a long delay will also result in a weak explosion due to reduced turbulence. This agrees with the experimental results shown in Fig. 3.

Effect of Ignition Timing Delay with Air Injection

The injection of air through the turbulence ring increases the turbulence intensity. The total turbulence intensity inside the sphere is made up of a transient component associated with the dispersion air jet and a steady component associated with the constant air flow through the turbulence ring. Figure 4 shows that the steady component helps maintain a strong explosion at longer time delays.

One may be tempted to explain these results by the suggestion that air injection helps keep the dust particles in suspension for a longer period of time. However, the settling velocity $V_\infty = \frac{2}{9} \frac{\rho_D R^2 z}{\mu_{air}}$ is only 0.7 cm/sec for starch particles whose average diameter is 15 μm. Visual observations confirm that noticeable settling occurs after only three or four seconds. Furthermore, it must be said that the bulk velocity of the injected air has no significant vertical component, by symmetry. It is therefore unlikely that this jet can oppose the settling of particles to any significant extent.

Effect of Turbulence

Figure 5 shows the effect of varying the rate of injection of air through the turbulence ring on the peak overpressure and the maximum rate of pressure rise. The experiments were run using two different concentrations, and the results are similar for each concentration.

The peak overpressure increases 45% from its value with no air injection to its highest value. Turbulence ensures that nearly all the oxygen available inside the vessel is consumed. What is much more remarkable is the increase in the maximum rate of pressure rise, which jumps from 2000 kPa/s with no air injection to over 8000 kPa/s at an injection rate of 4 grams of air per second, and drops back to around 6000 kPa/sec with injection at a higher rate.

It is well knwon that in pulverized coal boilers, where the particle size is of the order of 75 μm, combustion rates are aided by convection of oxygen to a particle due to the relative velocity between the fluid and the particle (Ref. 12). This effect cannot be as important for cornstarch particles of 15 μm size however. Consider a spherical particle of radius r_0, density initially at rest in a fluid and suddenly subjected to a flow set speed v_∞. The particle will pick up speed according to the formula

$$\frac{(v_\infty - v)}{v_\infty} = e^{-\frac{9}{2}\frac{\mu}{\rho r_0^2}t}$$

Small particles follow the flow very closely: a 15 μm starch particle will acquire 99% of the flow velocity in 3 ms.

Thus, it is reasonable to infer that the particles essentially follow the flow. That being the case, any inhomogeneity in dust concentration at the time of dispersion will be rapidly diffused by the microscale turbulence in the sphere, in the same way as dye particles were diffused in Reynolds dye experiment. This will tend to reduce the spread in the interparticle spacing and will have the effect of increasing the degree of homogeneity of fuel and oxidizer. All these factors combine to increase the burning velocity of the mixture and therefore, the maximum rate of pressure rise observed.

B) Experiments with Turbulent Methane-Air Mixtures

Because of the way in which the dust is dispersed in our combustion chamber and because of the way in which turbulence is induced, the turbulence intensity and the integral length scale of turbulence are expected to vary both in space and time. Measurement of these fundamental turbulence parameters, therefore, is not only difficult, but of limited value.

It was felt that an indirect way to characterize the turbulence in the combustion environment would be to study the propagation of methane-air flame in a flow field that replicated as closely as possible that of the dust-air flames.

Since the influence of turbulence on the burning velocity of methane-air mixtures has been extensively studied (Ref. 9), turbulence intensity can be recovered from correlations of u_t/u_e vs u'/u_e, for example, where

u_t = turbulent burning velocity,

u_e = laminar burning velocity,

u' = r.m.s. turbulent velocity.

Our dust combustion apparatus was therefore modified to study turbulent methane-air flames. The modified set-up is shown in Figure 6. In this set-up, the dispersion bottle was filled with a mixture containing 6% methane in air. The combustion chamber was exhausted to near vacuum, and then brought back up to atmospheric pressure by a mixture containing 6% methane in air injected through the turbulence mechanism described earlier. The methane came from a bottle, while the air came from the shop air supply. The two gases were metered by rotameters and intimately mixed in a specially designed chamber.

Figures 7 and 8 show the maximum pressure and rate of the pressure rise as a function of air mass flow rate. It is seen that the results follow the same trends observed in the dust combustion experiments and in the experiments on turbulent methane-air flames performed by Bradley et al. (Ref. 13).

While these preliminary results are encouraging, more work needs to be done before we can use these results as an input to the theoretical modeling of dust flames.

III. HYBRID COMBUSTION

Introduction

The explosion of hybrid mixtures of gaseous fuels and combustible dust with air is of particular interest in coal mine accidents where methane gas is usually present along with coal dust. The influence of inert dust on the combustion process is also of importance in mine accidents as rock dusting has become an accepted standard as an explosion suppressant.

There is much research being done currently on gas exposions and on dust explosions, but the subject of hybrid explosions has not been as extensively studied. Upward and horizontal propagation limits in methane-coal dust-air mixtures were investigated earlier by Singer[14] et al. Similar studies on lean limits have been conducted by Feng[10] et al. for coal dust and methane gas in a Hartmann bomb type of apparatus; by Bartnech[15] on PVC dust with methane and by Belmont[16] with PVC dust and propane. C.J. Dahn[17] investigated the effect on explosion strength of gasoline vapour on Refuse Derived Fuel and cornstarch.

On the otherhand, inerting coal dust air and methane-air explosions with rock dust as well as inhibitor dusts has been investiaged by Hertzberg[18] et al. It is of interest to note that the presence of small amounts of inert particles in a fuel air mixture can extend the lean detonability limits of gaseous fuels in air.[19] There is also literature available on the effect of powdered chemical inhibitors on gaseous flames which has been investigated by Van Tiggelen[20] and Mitani.[21]

A program has been initiated to investigate the mutual coupling between solid and gas phase combustion in a hybrid mixture. Experiments were done on methane-air mixtures with addition of varying amounts of inert dusts as well as combustible dusts. Also, the sensitization of dust explosions by the addition of small amounts of methane has been looked at.

In developing any new apparatus, it is necessary to determine the reliability by examining its ability to reproduce accepted results and its response to changing some of the basic apparatus parameters. This is especially important for apparatus that employ a different geometry or scale than others previously used. Prior to conducting explosion experiments, an adequate dust dispersion system had to be developed and tested. It was

decided that the apparatus would be a long combustion tube in the hope of generating a steady state combustion wave in a premixed dust air environment. For that reason, the tube length became limited to that in which adequate dispersion can be achieved and maintained for the duration of the explosion. Researchers at the University of Michigan and others have developed very long (400 m) tubes to study a steady state dust deflagration wave. However, this method relies on the flow ahead of the wave to entrain the dust layered on the floor. Thus, the problem of entrainment by an air blast of the dust on the floor is intrinsically coupled with the combustion problem. Furthermore, it is unreliable when lean mixtures are studied whereby the burning rate is slow, hence there will be no appreciable flow generated ahead of the flame and so no entrainment. Finally, this method requires a very strong ignition source to initiate a blast wave to generate a dust cloud and ignite it as well. Vertical flame tubes are also used in the study of dust and droplet explosions. However, it is felt that the typical diameter of these appratus (50 mm to 100 mm) is too small relative to the reported flame thickness. The tube diameter should be as large as the characteristic length scale of the flame. Dispersion in a large diameter vertical tube, however, is extremely difficult. Thus, the geometry selected for the new apparatus was to be a horizontal tube with a closed volume as outlined below.

Experimental Apparatus

The apparatus developed for these experiments is a long horizontal (LHT) tube, 0.3 m in diameter and 2.14 m long with 12 mm wall thickness as shown in Fig. 9. The total volume of the chamber is 0.156 m^3. The dust is distributed uniformly in a V-channel raised 38 mm above the floor of the tube. Prior to ignition, the dust is dispersed by 20 impulsively started jets emerging from a perforated shock tube (dispersion tube) which

runs the central axis of the appratus. The dispersion tube is 38.1 mm in diameter. The perforations on the dispersion tube are 4.7 mm in diameter and are uniformly spaced 100 mm apart. The jets are all oriented downward so that they impinge directly on the V channel. They are formed by rupturing a Mylar diaphragm between the dispersion tube and a pressurized driver section, located on the left hand side in Fig. 9. The driver section is pressured to 9.5 bar overpressure for all experiments. It is a 63 mm square cross section tube 0.51 m long with a volume of 2 liters or 1.3% of the test section volume. The duration of the jets is approximately 100 msec. The dust is ignited after a preset time from the rupture of the diaphragm, typically 85 msec. The ignition source is weak, consisting of a 0.076 mm brass wire 25 mm long connected to a 115 V A.C. source. For mixtures that were difficult to ignite, the ignition source was augmented by wrapping some fine magnesium filaments around the brass wire to produce a flashbulb effect. There are eight threaded ports spaced 0.3 m apart along an axis of the test section to which instrumentation may be attached. There is also an additional port 100 mm from the end near the driver section to provide more flexibility to the igniter location.

For all experiments, the gaseous mixture is loaded into the test section by the flow through method for 20 minutes so that the total volume is five times the test section. The flow rates are regulated by a set of calibrated rotameters so that the fuel air concentration can be varied. The driver section is loaded with the same mixture as the test section by the method of partial pressure.

Pressure time histories can be measured with a PCB piezoelectric pressure transducer mounted midway along the length of the tube. Flame arrival times can be recorded by ion probes mounted to its various port

locations. The probe measurements are recorded on storage oscilloscopes.

Two methods were used to assess the quality of the dust dispersion in the long horizontal tube. First, the dispersion was observed out of the tube. Although the resulting cloud appeared to be spatially uniform, the human eye is not very sensitive in judging concentrations. Since an optical probe was not available at the time, it was decided to compare combustion results to those of others that are believed to be accurate. Figure 10 shows the maximum explosion pressures obtained using the LHT for various concentrations of cornstarch dust. Shown on the same graph are the results of tests made in the 330 ℓ spherical bomb also at McGill and those done originally by Hartmann et al.[22] in a Hartmann bomb. The results from the LHT are in very good agreement with those of the 330 ℓ sphere except for a 12% discrepancy at the higher concentrations. The curve follows the same trend as that of Hartmann, except the latter are uniformly 20% higher. This is most likely due to the difference in particle size and the moisture content of the fuels. It appears that the maximum pressure is developed at a concentration of 600 g/m^3 which is nearly 2.25 the calculated stoichiometric concentration based on the cornstarch approximate chemical composition $C_6H_{10}O_5$. The maximum overpressure developed at this concentration is 6.8 bar, although 7.8 bar is reported in the large spherical bomb. This value is close to that of pure methane in air at the stoichiometric concentration as exhibited in Fig. 11.

Tests were run with methane in air without any dust for comparison purposes. For these runs a simulated dispersion was used, that is the driver section was pressurized and the gas was ignited 85 ms after the rupture of the diaphragm. This was done to ensure that the same kind of turbulent environment was present as is in a dust experiment. Figure 11 shows the maximum overpressure versus concentration. The circles represent

actual data points, whereas the solid line the theoretical adiabatic value based on equilibrium calculations. The maximum value is achieved at a concentration of 10% by volume which corresponds to an equivalence ratio of 1.05. At this point, the theoretical and experimental values are the same. However, as the mixture is made more lean, the experimental value becomes lower than the theoretical one. At a concentration of 6%, 4.6 bar overpressure is achieved, whereas 5.5 bar is predicted. This can be attributed to the more significant heat losses to the wall of the tube for the lean mixtures which have a lower laminar burning velocity. At the ignitable limit, with the weak igniter this deviation is 18%. The effect of the non-adiabacity associated with the slow flames is further brought out by noting that when a quiescent mixture of 9.5% CH_4 is burned, the resulting overpressure is only 6.7 bar, wich is 16% below the theoretical. The quiescent mixture burned at a rate 25% slower than the turbulent mixture. Slower burning flames have prolonged contact with the cold boundary, hence higher heat losses.

A) Effect of CH_4 on Dust Explosions

A series of tests were done admixing small amounts of methane gas below the lower explosive limit, to an explosive mixture of dust and air. Two dust air mixtures were examined, 300 g/m^3 cornstarch and 600 g/m^3 cornstarch. Cornstarch was selected as a fuel because it has good particle size uniformity near 15 μm and it consists mostly of volatiles with very little fixed carbon or ash. It is also readily available in pure form and is inexpensive. The lower concentration, 300 g/m^3 represents a lean mixture, whereas the higher concentration is representative of rich mixtures, based on the explosion pressure developed, as seen in Fig. 10.

The explosion pressure is shown in Fig. 12 plotted against the percentage by volume of CH_4 added to the two dust air mixtures considered. Three methane concentrations were used: 2%, 4% and 6%. The latter is the ignitable limit with our weak ignitor, however, once ignited, it is capable of supporting horizontal propagation of a flame. The results show little change for the 600 g/m^3 dust air mixture. With no methane, the peak pressure developed is 6.5 bar and climbs to an asymptotic value of 7.0 bar at 6%. This asymptote is maintained until the concentration of methane admixed reaches stoichiometry, after which quenching occurs by the same methods as in rich gas-air mixtures. The asymptotic value exists because the the maximum pressure developed is limited by the amount of oxidizer available for reaction with the fuel. The maximum value of 7 bar is slightly less than the maximum for methane only due to additional radiation losses and other thermal losses by the particles.

The leaner mixture of dust and air, 300 g/m^3, exhibits the same kind of behaviour. With no methane present, the peak pressure is 5 bar, and this value increases slowly with the concentration of CH_4 admixed. At 6% CH_4 the pressure developed is still slightly less than that of the rich dust-air mixture, however the same asymptotic value is reached with 9% CH_4. Thus, it appears that for dust air mixtures in the region between the lean and saturated regions, admixing of small amounts of methane gas causes slight increases in peak overpressure, and the maximum overpressure possible is limited by the amount of oxidizer present. When the concentration of methane gas present is flammable by itself, other factors are of influence and these will discussed later.

Also of importance in dust explosions is the time of explosion. Figure 13 shows the burnout time for the tests as a function of methane

concentration. The burnout time is measured from ignition to 95% of the peak pressure. The peak pressure is not used because the slope at the top of the pressure-time trace is nearly flat, as indicated in Fig. 14.

As shown in Fig. 13, although the peak pressure is only slightly affected, the burnout time (τ_b) is more markedly affected by the presence of small amounts of CH_4. With no methane, the burnout time is 200 msec for 300 g/m^3 and 195 msec for 600 g/m^3 cornstarch in air. With an addition of 2% CH_4 this drops to 140 msec for the 600 g/m^3 mixture and to 150 msec for the 300 g/m^3 mixture or a reduction of 30% and 25% respectively. Further increase in CH_4 content to 6% causes a total reduction of τ_b of 38% and 36% for the rich and lean mixture, respectively. The burnout time thus indicates that the average explosion time is reduced by addition of a premixed combustible gas, indicating that the overall reaction rate must be increased.

Another indication of this is to look at the K_{ST} factor which is a measure of the maximum local burning rate. It is defined as $(\frac{dP}{dt})_{max} L_{CHAR}$, where $(\frac{dP}{dt})_{max}$ is the maximum burning rate of pressure rise and L_{CHAR} is the characteristic length of propagation of a flame in the apparatus. Figure 15 is a plot of K_{ST} versus the methane concentration for the two dust air mixtures. Note the rapid increase of K_{ST} from 118 bar m/sec to 200 bar m/s for 600 g/m^3 dust concentration with 2% methane admixed. Further increase in the methane concentration up to 6% results in a less dramatic increase in K_{ST} to a value near 220 bar m/s. The curve for 300 g/m^3 is similar except the trend is less severe.

Also indicative of the change of reaction rate is the measured flame speed as seen in Fig. 16. These were done by measuring the time of arrival of the flame by two ion probes spaced 0.9 m apart at the mid-

section of the tube. At this region the rate of pressure rise is nearly constant so that the flame speed can be assumed as also being constant over the same interval. The curve shows the same upward trend of the flame speed with increased methane concentration, indicating higher reaction rates. Notice that the flame speed rises quickly with the initial addition of 2% CH_4 and then further addition to 4% causes only a mild increase. However, at 6% CH_4 the gas mixture is capable of sustaining combustion wave on its own and the flame speed increases again.

B. Dust in Methane-Air

When the gas concentration is increased sufficiently, the dominant mechanism in the hybrid explosion is the gas phase combustion. The question now is what is the effect of dust on a near stoichiometric premixed methane-air flame? The tests were done with 9% CH_4-air mixtures and three different types of dust, one inert, and two types of fuel dust: i) Alumina ($A\ell_2O_3$) with particle size in the range of 5 μm - 9 μm is used as an inert dust, ii) cornstarch with particle size in the range of 15 μm - 20 μm, and iii) coal from Devco #26 mine from Nova Scotia with particle size of a broad distribution under 73 μm (#200 mesh), were used as combustible dusts. All three dusts acted as retardants to the methane air flame as can be seen in the following figures. Figure 17 shows the peak explosion pressure developed against the dust concentration present for all three dusts. Coal dust caused the greatest reduction in peak pressure from 7.6 bar with no dust to 5 bar with a high concentration, 800 g/m^3. However, this is still not significant as an inhibitor with respect to the standards of the U.S. Bureau of Mines.[18] Alumina shows slightly less retardation effect and the cornstarch almost none. Note that for all three dusts, the curves seem to level off above 400 g/m^3 and increasing the

concentration to 800 g/m^3 produces little additional effect.

Although the dusts produce little effect in reducing the explosion pressure, they are efficient in retarding the reaction rate by increasing the burnout time by as much as a factor of 4 as shown in Fig. 18. Coal dust which produces only a 35% reduction in peak pressure significantly slows down the reaction rate. The curve is steep at first and tends to level off at the higher concentrations. The same trend is visible for the other dusts. Cornstarch which is very ineffective in reducing the peak pressure is capable of retarding the flame to a significant degree. Alumina was the least effective yet it is still significant, doubling the bournout time from 65 msec to 140 msec. The local rate of pressure rise, or the K_{ST} factor is similarly affected (Fig. 19). It is reduced from 400 bar m/sec for 9% methane air with no dust to 90 bar m/sec with 800 g/m^3 of coal, and alumina, and 120 bar m/sec for cornstarch. All three curves tend to level off at the higher concentrations to a minimum value near 90 bar m/sec. The measured flame speed curves are almost identical as shown in Fig. 20 and they reflect the reduction in reaction rate by showing marked decrease in flame speed from 41 m/s for pure methane in air to 10 m/s when there are high dust concentrations present.

It is apparent then that both inert and combustible dust can act to retard a stoichiometric methane air mixture. Though the explosion pressures are only mildly suppressed, the rates of pressure rise are significantly reduced.

C. Experiments with Mixtures of Cornstarch and Ferric Oxide

It is felt that observing the effect of adding a small proportion of different inert dusts to a combustible dust-air mixture may be a fruitful

means of investigating how a dust flame propagates. In particular, studying the decrease in the maximum overpressure and maximum rate of pressure rise observed when two different inert dusts with different radiative properties are successively mixed with the same combustible dust-air mixture may enable us to assess the relative importance of radiation and diffusion as modes of energy transport.

Suppose that dusts A and B are both chemically inert, have equal thermal conductivities and capacities, but differ substantially with regard to their radiative properties, e.g., A might be a transparent dust, while B is opaque. If a certain amount of dust A is mixed with a combustible dust-air mixture and the resulting mixture ignited, the explosion will produce a lower peak pressure than a pure combustible dust-air explosion because: a) some thermal energy released during combustion will be soaked up by the inert dust, b) owing to this energy absorption by the inert dust, flame propagation will be retarded and the radiation loss to the wall during the explosion, which is proportional to the duration of the explosion, will be increased. Now, if an equal amount of opaque dust B is mixed with the combustible dust-air mixture, the resulting explosion will peak at an even lower pressure than with A above: dust B will absorb thermal energy in the same amount as did dust A, but because of its opacity, it will impede flame propagation even more than A and the wall loss will be greater. How much more depends critically on the importance of radiation as a mode of energy transfer in the propagating flame.

Thus, the important and controversial question of radiative transport may be addressed indirectly via the study of inert plus combustible dust-air mixtures. As a first step in this direction, the following experiment was made in our 333 liter sphere.

A constant charge of 100 grams of cornstarch dust was intimately mixed with variable amounts of ferric oxide (Fe_2O_3) powder of 6 micron average diameter. One gram of CAB-O-SIL was added to this mixture as a fluidizing agent. The mixture was dispersed into the sphere using the mechanism described before. After a delay of 0.5 seconds, the mixture was ignited by means of an exploding wire.

Figure 21 shows the maximum pressure developed and maximum rate of pressure rise as a function of Fe_2O_3 concentration (defined to be the mass of Fe_2O_3 divided by the mass of cornstarch). The maximum pressure varies with the Fe_2O_3 concentration according to the approximate relation

$$P_{max} = 117 - 3.04[Fe_2O_3].$$

The portion of the pressure decrease associated with thermal energy absorption by ferric oxide can be approximated in the following manner.

The approximate formula $C_6H_{10}O_5$ for cornstarch (Ref. 11) yields the stoichiometric equation

$$C_6H_{10}O_5 + 6(O_2 + 3.76\ N_2) \rightarrow 6\ CO_2 + 5\ H_2O + 6 \times 3.78\ N_2$$

Assuming that little chemical energy is stored in the C - H_2O bonds of cornstarch, the energy balance is

$$6\ u_f(C) + 5\ V_f^\circ(H_2O)_\ell + 6\ V_f^\circ(O_2) + 6 \times 3.76\ V_f^\circ(N_2) =$$

$$6\ V_f^\circ(CO_2) + 5\ V_f^\circ(H_2O)_2 + 6 \times 3.76\ V_f^\circ(N_2) + V_r$$

$$u_r = 555.26 \text{ kcal/mole } C_6H_{10}O_5.$$

If the added Fe_2O_3 comes into thermal equilibrium with the product gases, we have

$$u_r = 6u_o^{T_f}(CO_2) + 5V_o^{T_f}(H_2O) + 6 \times 3.76\ V_o^{T_f}(N_2) + M_{Fe_2O_3}V_o^{T_f}(Fe_2O_3)$$

Introducing perfect gas assumptions and differentiating with respect to $u_{Fe_2O_3}$:

$$U_r = 6C_{v_{CO_2}}(T_f - T_o) + 5C_{v_{H_2O}}(T_f - T_o) + 22.56\ C_{v_{N_2}}(T_f - T_o) +$$

$$M_{Fe_2O_3}\ C_{v_{Fe_3O_3}}(T_f - T_o)$$

$$0 = (6C_{v_{CO_2}} + 5C_{v_{H_2O}} + 22.56\ C_{v_{N_2}} + M_{Fe_2O_3}C_{v_{Fe_2O_3}})\frac{dT_f}{dM_{Fe_2O_3}} + (T_f - T_o)C_{v_{Fe_2O_3}}$$

$$\frac{dT_f}{dM_{Fe_2O_3}} = \frac{-(T_f - T_o)C_{v_{Fe_2O_3}}}{(6C_{v_{CO_2}} + 5C_{v_{H_2O}} + 22.56\ C_{v_{u_2}} + M_{Fe_2O_3}\ C_{v_{Fe_2O_3}})}$$

Now $P_f = \Sigma\ P_{gf} = \Sigma\ n_g\ \mathbb{R}\ T_{gf}/v$

where g refers to each gaseous product component, $\mathbb{R}$ is the universal gas constant and V is the volume of the vessel.

Hence $$\frac{dP_f}{dT_f} = \frac{33.56\ \mathbb{R}}{V}$$

$$\frac{dP_f}{dM_{Fe_2O_3}} = \frac{dP_f}{dT_f}\frac{dT_f}{dM_{Fe_2O_3}} = \frac{-33.56\ \mathbb{R}(T_f - T_o)C_{v_{Fe_2O_3}}}{V(6C_{v_{CO_2}} + 5C_{v_{H_2O}} + 22.56C_{v_{N_2}} + M_{Fe_2O_3}C_{v_{Fe_2O_3}})}$$

Since the Fe_2O_3 concentration is small, we can neglect the Fe_2O_3 term in the demonstrator. Upon substituting the gaseous properties and the flame temperature calculated for zero Fe_2O_3 addition, we obtain

$$\frac{dP_f}{dM_{Fe_2O_3}} = -0.15 \text{ psi/\% } Fe_2O_3$$

Thus, the observed decrease in the maximum pressure is 20 times that arising from thermal energy absorption by the Fe_2O_3 alone.

In the near future, it is planned to study the effect of adding different grades of silica (SiO_2) to the cornstarch-air mixture. It is well known that spraying rock dust on the floor of mine galleries is a standard means of reducing the risk of a coal dust explosion. This part of our program has the additional aim of identifying properties of an inertant dust which makes it effective or ineffective as an inhibiting agent.

IV. DUST FLAME ACCELERATION

A. General Remarks

A study of flame acceleration in dust-air mixtures due to obstacles is being carried out at McGill and the present section describes the preliminary results obtained.

It is well known that when obstacles are placed in the path of the gas flame front, the gas flame can be accelerated.[24] In practice, there are usually many pieces of equipment present where accidental gas or dust explosions occur. The pressure wave associated with the accelerated flame can cause significant structural damage.

However, the different mechanisms of dust flame propagation and acceleration are still unknown.[25] Hence, fundamental as well as phenomenological studies of dust flame acceleration are important.

As discussed in Ref. 26, a typical gas flame has a thickness of the order of about 1 mm. If the gas flame propagates with uniform velocity the flame front surface is smooth, but when obstacles are placed in the path of the flame, a velocity gradient is produced, which changes local velocity and folds and wrinkles the flame surface resulting in flame acceleration.

A dust flame is typically two orders of magnitude thicker than flame.[4] In consequence, dust flame acceleration must be quite different from gas flame acceleration. It seems impossible for the velocity gradient to intensely influence such a thick flame zone. Thus, the fundamental mechanism by which turbulence generated by obstacles influences and accelerates dust flame propagation is unknown at present.

Since a dust flame is thick, a long vertical test tube is needed for the study of dust flame acceleration. The diameter of the tube is an important factor which effects the flame speed. Compared with the thickness of the dust flame zone, small diameter tubes cannot produce useful results. On the other hand, a large diameter tube is difficult to implement in the laboratory. Thus, a middle sized test tube is used with a diameter of 0.15 meter and length about 2 to 3 meters.

B. Dust flame Acceleration: Apparatus and Preliminary Results

Getting a uniform dust dispersion along a long vertical tube involves many difficulties. Uniform dust dispersion is essential because

without this uniformity any resulting data are apparatus dependent and lead to a lack of universal validity. Hence, our first step lies mainly in testing and designing dust dispersion techniques for dispersing the dust in a vertical tube.

One technique of dust dispersion which has been tested uses a mechanical dust feeder with fluidization in a continuous flow system which uniformly enters from the bottom of the tube, as shown in Fig. 22. The measured data including flame speed and pressure in the experiments, both with and without obstacles is shown in Figs. 23a and 23b.

Figure 23 shows that for a dust flame speed of 30 m/sec, $(\frac{dP}{dt})_{max}$ is 47 bar/sec when dust concentration is 0.2 oz/ft^3. Obstacles with the ratio of the diameter of obstacle to the distance of each obstacle being 1/6 increases the speed of the flame front to 100 m/sec, and $(\frac{dP}{dt})_{max}$ to 127 bar/sec. Measurements of flame temperature by thermocouple gauges are shown in Fig. 24.

Figure 24 shows three temperature trace cross-sections x_1, x_2 and x_3 respectively, and one pressure trace for cross-section x_p. The speed of flame front is about 34 m/sec, as determined by the starting points of three temperature traces. The time required for the flame front to pass through the whole test tube is almost 60 ms, and the duration of combustion in each cross-section is longer than 120 ms. Since the burning time anywhere in the tube is almost twice the time the flame takes to propagate along the whole tube, then at the end of the propagation process, the entire volume continues to burn until exhaustion.

The advantage of the dust dispersion system used here is that the low speed air flow (1 m/sec) can suspend a vry narrow particle distribution and this can be calculated, based on Stokes theory of drag on a sphere. In

addition, the low air flow speed produces very weak initial turbulence. This is a remarkable advantage in the study of flame acceleration due to turbulence.

The problem in this system is that processing the dust with the narrow size distribution required is too expensive to practise. Also, at a given cross section of the test tube there is a speed profile of air flow causing some dust to fall down as well. These factors influence the uniformity of dust dispersion. The dust concentration in the test tube is not easy to change because it depends on the speed of air flow and the speed of mechanical feeder. Finally, the operation of the dust dispersion system is rather cumbersome.

C. Refinement of the Dust Flame Acceleration Experiment

One of the important problems in dust flame acceleration experiments is treating a dust cloud that is uniform in both space and time. The experiment not only requires uniform spacial distribution of the particles along the tube axis, but the particles must remain suspended for the duration of the explosion. The duration is in turn a function of the length of the tube and the speed of the flame front. For a 5 meter long tube in which the flame travels at 10 m/s, this time is 0.5 seconds. If the particles are below 30 μm diameter, the settling velocity due to the action of gravity is of the order of 0.2 m/s and is negligible compared to the flame speeds.

In order to obtain a uniform axial distribution, another technique being developed is to cascade a long vertical tube by a series of segments. Each segment contains its own dust dispersion system and has the same contruction as the others as shown in Fig. 25. With this configuration, the global non-uniformity along the length of the tube is negligible. The

dispersion within each segment of the tube may be refined by using the following techniques.

Figure 26 shows the structure of a segment. It consists of a 150 mm diameter tube 0.6 m long. A 12.5 mm dispersion tube runs along the wall of the tube, containing small dispersion holes (1 mm to 2 mm diameter) aligned with the tube diameter. In front of the dispersion tube there is a 9.5 mm circular cross section bar to deflect the dust jets. The dispersion tube is connected upstream to a ball valve, a small cavity, a solenoid valve and a small air reservoir respectively, as seen in Fig. 26. Prior to dispersion, a measured quantity of dust is loaded into the small cavity between the dispersion tube and the solenoid valve. The air reservoir is 50 cm^3 and is pressurized to 10 bar overpressure. When the solenoid valve is opened, the dust is convected from the cavity through the dispersion tube. The impulsive jets emerging from the dispersion holes blow the dust uniformly throughout the test tube. Experimental results show that proper proportioning of the dispersion elements ensures a uniform distribution throughout the length of a segment. The details of the testing procedure of the dispersion system are given in Appendix B.

D. Interpretation of Burning Velocity of a Dust Flame

As mentioned previously, the dust burning zone observed in our 2 meter long, 150 mm diameter test tube is unstable and grows to the total length of the tube in the explosion process. When the dust flame front reaches the top there is global burning within the whole tube. In this case, it is difficult to apply the concepts and analysis associated with gas flames. In the analysis of gas flame acceleration, it is assumed that the burned and unburned regions are demarcated by the flame. This is because the flame is considered to be very thin, of the order of fractions

of a millimeter. Figure 27 illustrates this concept. This way, the location of the gas flame can be related to the burned mass (Eqn. 1) and the burning rate (Eqn. 2). The burning rate in this case is defined in Eqn. 3 if we assume that the process is isobaric and the unburned gases are compressed isentropically (Eqn. 4). The relation between flame location and unburnt mass is given by:

$$\frac{m_u}{m_o} = (1 - \frac{m_b}{m_o}) = \frac{1}{m_o}\frac{\pi}{4} D^2(H - h)\rho_u \qquad (1)$$

The relation between the gas flame location and the burning rate is:

$$S = \frac{dh}{dt} - \frac{H - h}{p^{\gamma_u}} \frac{dp}{dt} \qquad (2)$$

By definition, the burning rate S is

$$\frac{dm_u}{dt} = - A_f \cdot \rho_u \cdot s \qquad (3)$$

$$A_f = \pi D^2/4$$

In an isentropic compression process:

$$\frac{p}{\rho_u^{\gamma_u}} = \text{const.} \qquad (4)$$

Equations 1 and 2 show that the data of gas flame location with respect to time, which are measured in the gas flame acceleration experiments, cannot be treated only as independent characteristic parameters for studying the acceleration process, but also can be related to the explosion pressure to obtain the burning rate (i.e., in general say, normal combustion velocity). As far as dust flame acceleration is concerned, maybe it is possible that in very long test tubes (i.e., longer than 20 meters), the

usual concepts and analyses for gas flame propagation are still applicable under the condition that stable dust burning zone is achieved. Generally, in a test tube with limited length, a stable dust burning zone is not easy to achieve. In this case, the location of dust flame-front has no relation to the burnt mass of dust-air mixture and the dust burning rate. The data of the locations of dust flame-front measured in the experiments are useless for getting any characteristic parameter related to the acceleration process of dust explosion.

Another important problem, aside from achieving a uniform dust dispersion being raised in our study of dust flame acceleration is the following: What characteristic parameter can be used to describe the global phenomenon of dust flame acceleration?

An equivalent burning velocity may be such as the characteristic parameter as defined in Eqn. 5:

$$S(t)_{equivalent} = \frac{1}{\frac{(P(t))}{P_o}^{1/\gamma_u}} = \frac{H}{(P_{max} - p(t))} \frac{dp(t)}{dt} \qquad (5)$$

It can be derived from

$$\frac{p - p_o}{p_{max} - p_o} = \frac{m_b}{m_o} = \frac{m_o - m_u}{m_o} \qquad (6)$$

with Eqns. 3 and 4 shown before.

Equation 6 shows the relation between dust explosion pressure and burnt dust mass. Corresponding to the amount of burnt dust, an equivalent dust flame can be imagined to exist in the dust burning zone. The variation of the equivalent burning velocity with respect to time (t) can be obtained from the experimental data of pressure change with time (t).

A closed test tube is necessary to measure maximum pressure. Some phenomena of dust burning zone may be analyzed from the data of equivalent burning velocity change with time. Experimental and analytical research using equivalent burning velocity to study dust flame acceleration is being carried out at McGill now.

REFERENCES

1. Hartmann, I., Cooper, A.R. and Jacobson, M.: Recent Studies on the Explosibility of Cornstarch, U.S. Bureau of Mines Rept. of Inv. No. 4725, 1951.

2. Bartknecht, W.: Explosions - Course - Prevention - Protection. Translated by H. Burg and T. Almond. Springer-Verlag, New York, 1980.

3. Field, P.: Dust Explosions. Handbook of Powder Technology, Vol. 4. Elsevier, 1982.

4. Swift, I.: Developments in Dust Explosibility Testing: The Effect of Test Variables. Paper presented at the International Conference on Fuel-Air Explosions held at McGill University, Montreal, Canada, November 4-6, 1981.

5. Kaufman, C.W.: Agricultural Dust Explosions in Grain Handling Facilities. Paper presented at the International Conference on Fuel-Air Explosions held at McGill University, Montreal, Canada, November 4-6, 1981.

6. Wolanski, P.: Fundamental Problems of Dust Explosions. Paper presented at the International Conference on Fuel-Air Explosions held at McGill University, Montreal, Canada, November 4-6, 1981.

7. Marks' Standard Handbook for Mechanical Engineers. Baumeister, Avallone and Baumeister, eds., 8th ed. McGraw-Hill, 1979.

8. Nagy, J. and Portman, W.M.: Explosibility of Coal Dust in an Atmosphere Containing a Low Percentage of Methane. U.S. Bureau of Mines Rept. of Inv. no. 5815, 1961.

9. Abdel-Gayed, R. and Bradley, D.: The Influence of Turbulence upon the Rate of Turbulent Burning. Fuel-Air Explosions, University of Waterloo Press, 1982.

10. Hertzberg: Private Communication

11. CRC Handbook of Chemistry and Physics, 60th ed. Chemical Rubber Co., Cleveland, 1980.

12. Nagy, J., Seiler, E.C., Conn, J.W. and Verakis, H.C.: Explosion Development in Closed Vessels. U.S. Bureau of Mines Rept. of Inv. no. 7507, 1971.

13. Abdel-Gayed, R. and Bradley, D.: A Two-Eddy Theory of Gaseous Combustion. Proc. Roy. Soc. of London, 1980.

14. Singer, J.M.: Limits of Flame Propagation of Coal Dust-Methane-Air Mixtures, U.S. Bureau of Mines RI 7103 (1968).

15. B.G.-Chemie: Richtline Nr. 4: Statisch Elektrizitat (new ed. 1971).

16. Pellmont, G.: Explosion-und zundverhalten von hybriden Gemishen aus brennbaren stauben und bunngasen, Dissertation ETH, Zurich Nr. 6498 (1979).

17. Dahn, C. James: Flammable Vapor Contribution to Dust Explosions, Safety Consulting Engineers Inc., Rosemount, Illinois 60018.

18. Hertzbergh, M., Cashdollar, K., Lazzara, C., Smith, A.: Inhibition of Coal Dust and Methane Explosions", U.S. Bureau of Mines, RI 8708 (1982).

19. Wolanski, P., Adams, P., Maker, B., Kauffman, C., Nicholls, J.: Dusty Gas Detonations. Paper presented at 1982 Fall Technical Meeting of Eastern States Section of the Combustion Institute.

20. Van Tiggelen, A., Combustion and Flame 8:257-266 (1964).

21. Mitani, T., Niioka, T., Combustion and Flame 55: 13-21 (1984).

22. Hartmann, I., Cooper, R., Jacobson, M., U.S. Bureau of Mines RI 4725.

23. Feng, K.K.: Hazardous Characteristics of Canadian Coal Dusts. Energy Research Program, Division Report ERP/MRL 82-132(OP)(J).

24. Lee, John H.S.: Phenomenology of Gas Explosions. Note Book (1980).

25. Field, P.: Dust Explosions. Handbook of Powder Technology Vol. 4 (1982).

26. Lee, John H.S.: Overview of Gas Explosions and Recent Results in the Study of Turbulent Deflagrations and Detonation (1983).

27. Smoot, L.D. and Pratt, D.T.: Pulverized Cool Combustion and Gasification. Plenum Press (1979).

TEST APPARATUS
(V = 0,333 m³)

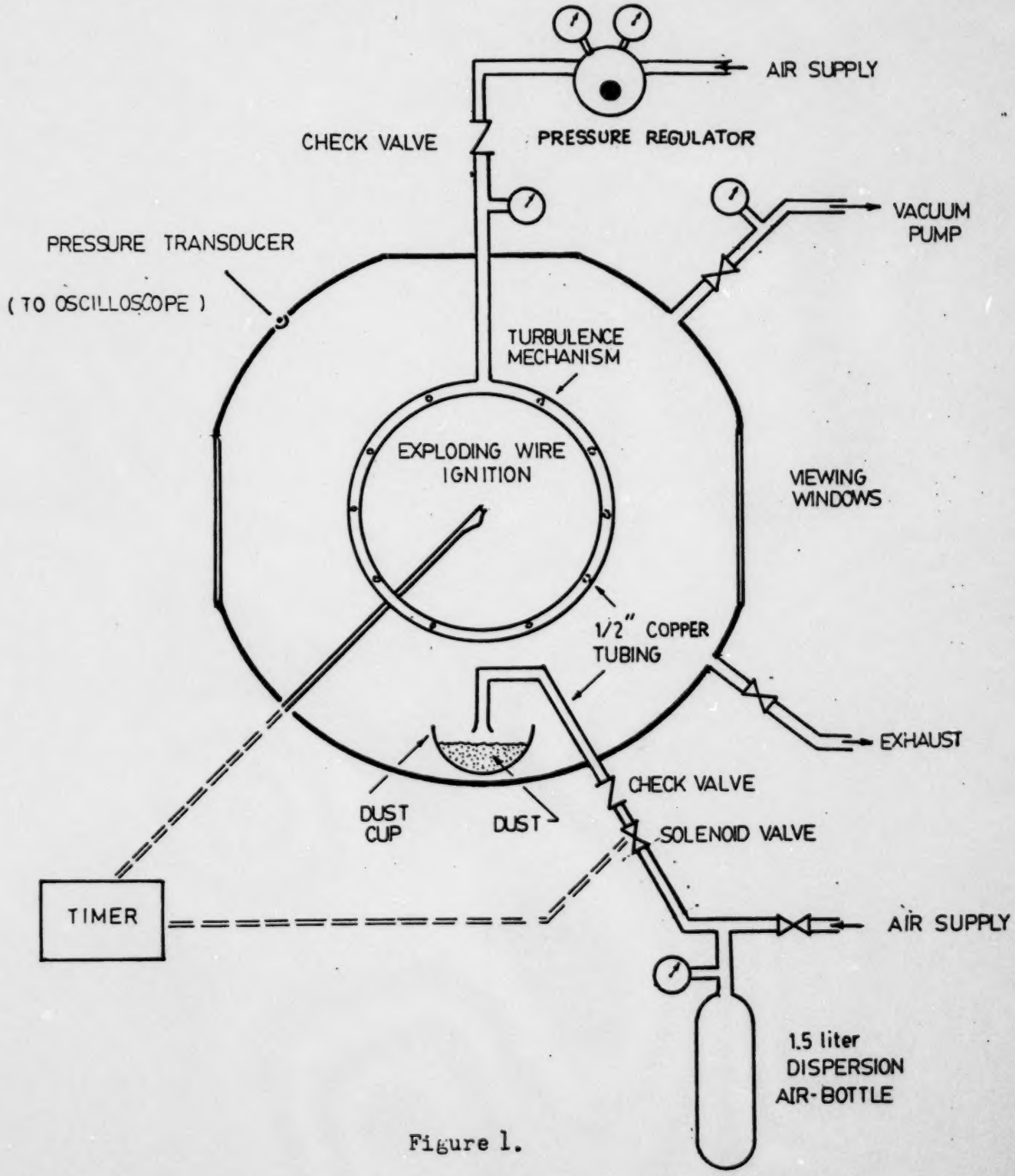

Figure 1.

MAXIMUM OVERPRESSURE vs. AVERAGE CONCENTRATION

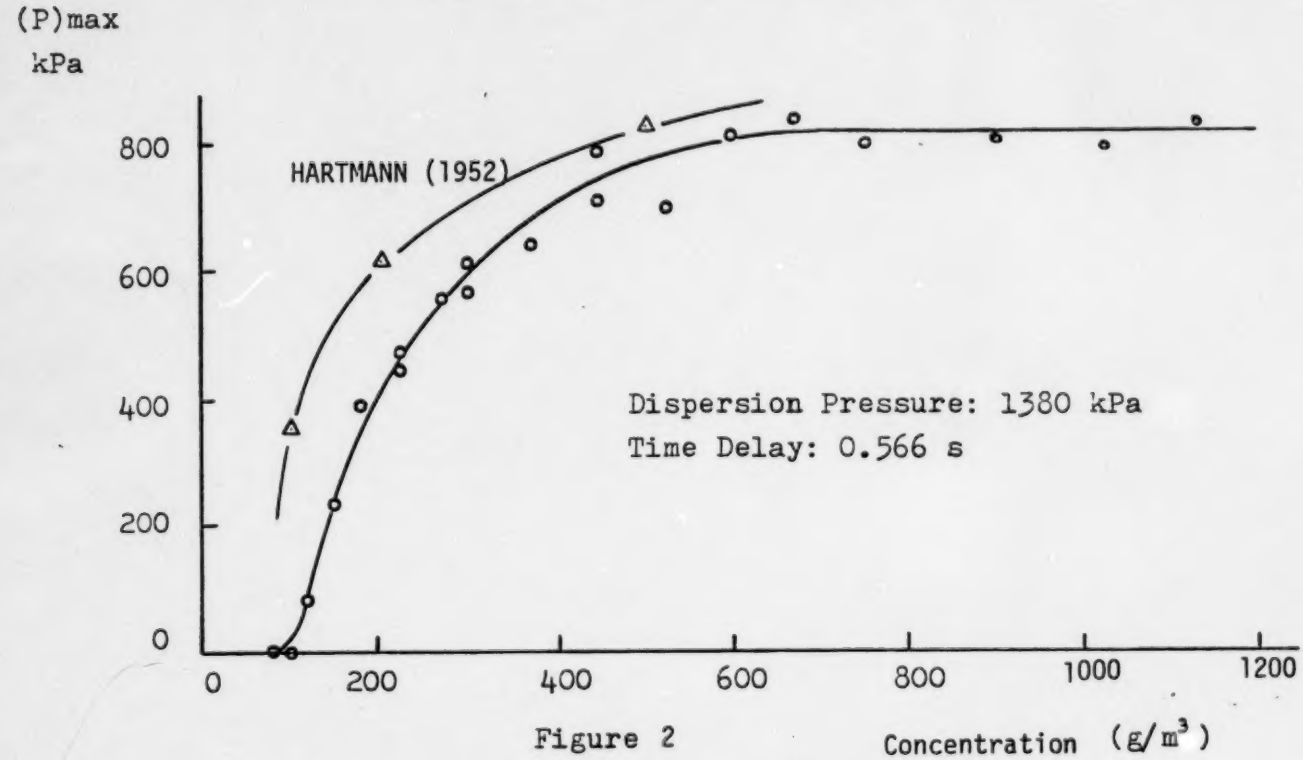

Figure 2

MAXIMUM RATE OF PRESSURE RISE vs. AVERAGE CONCENTRATION

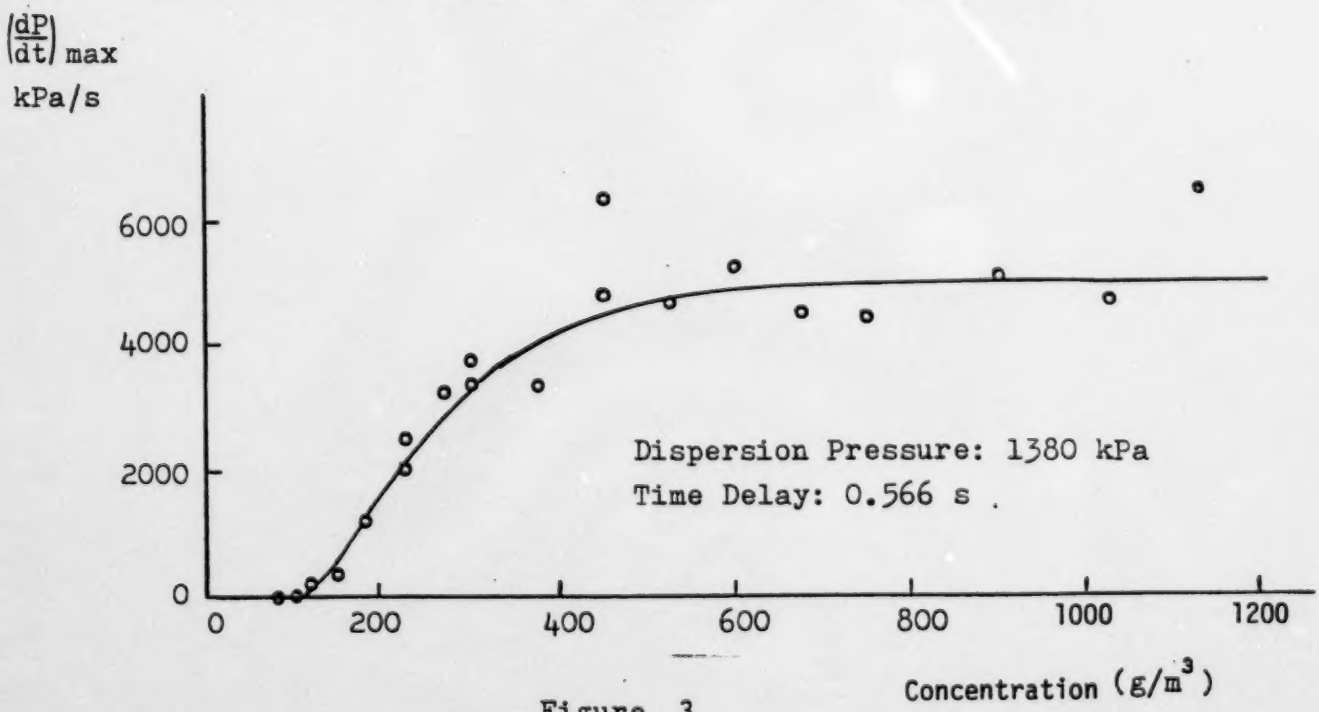

Figure 3

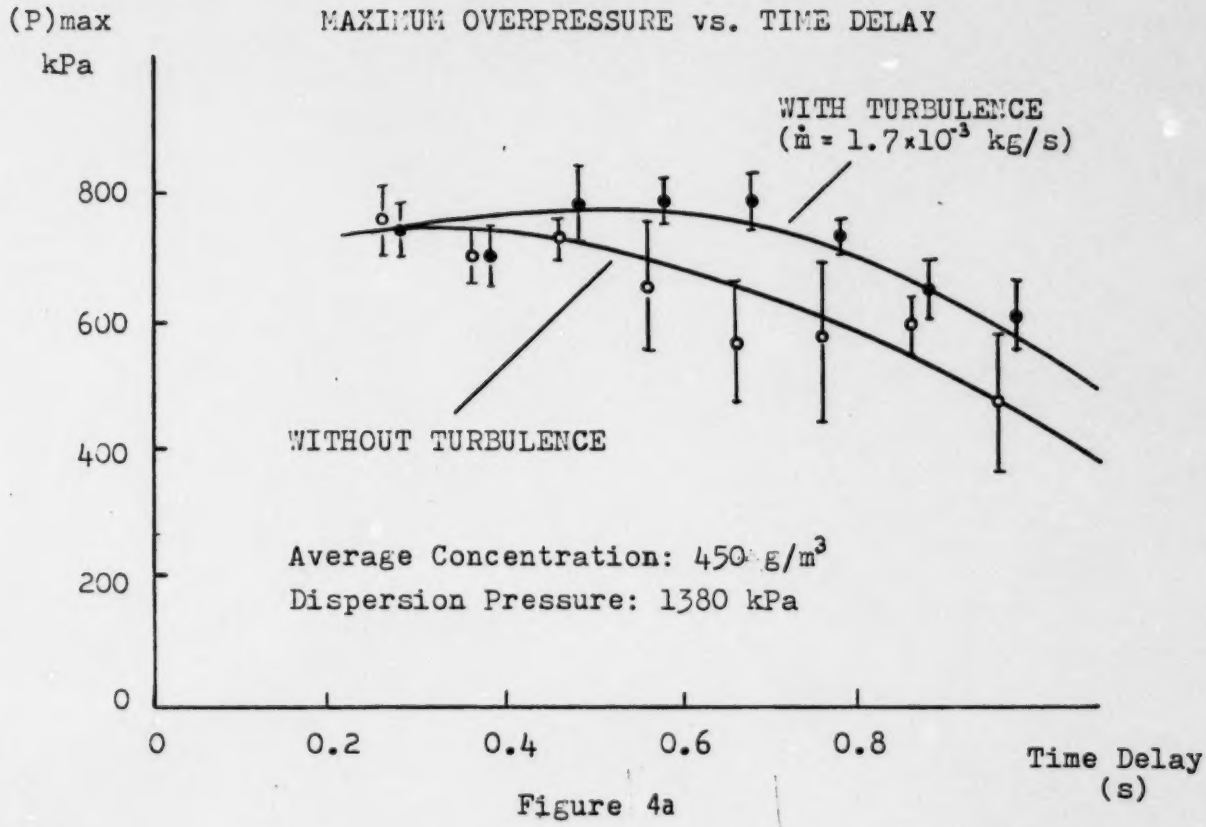

Figure 4a

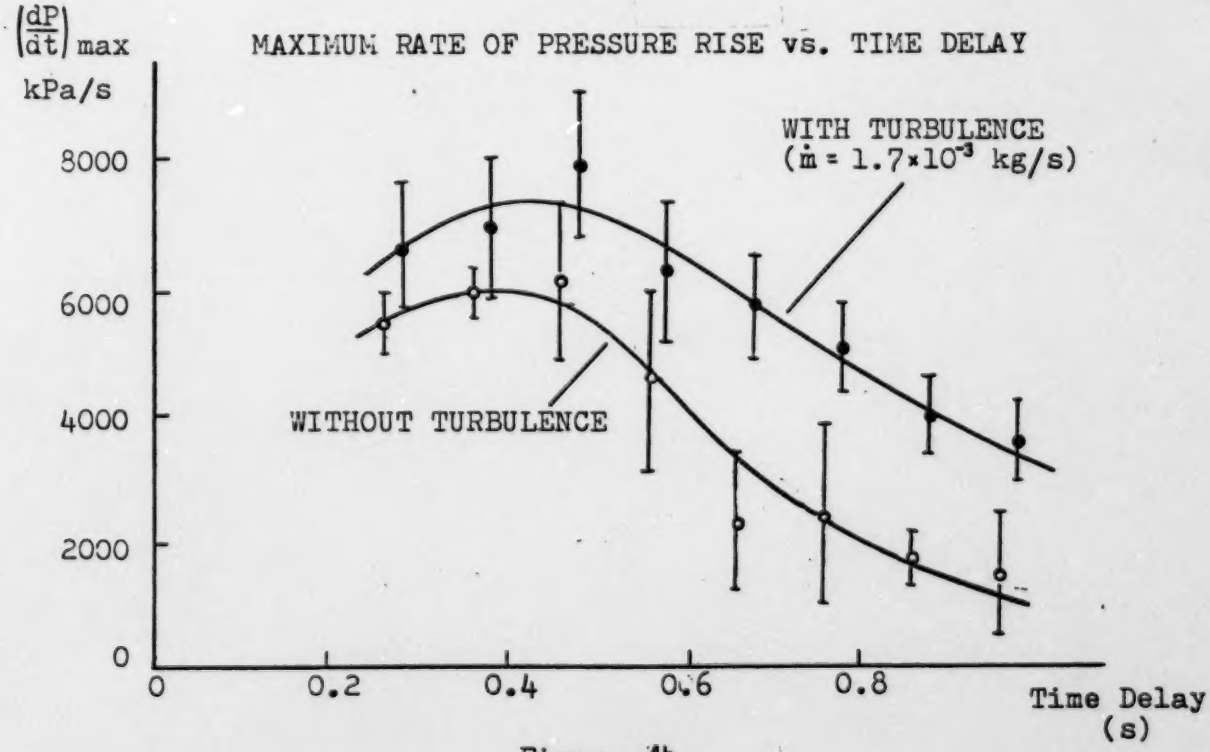

Figure 4b

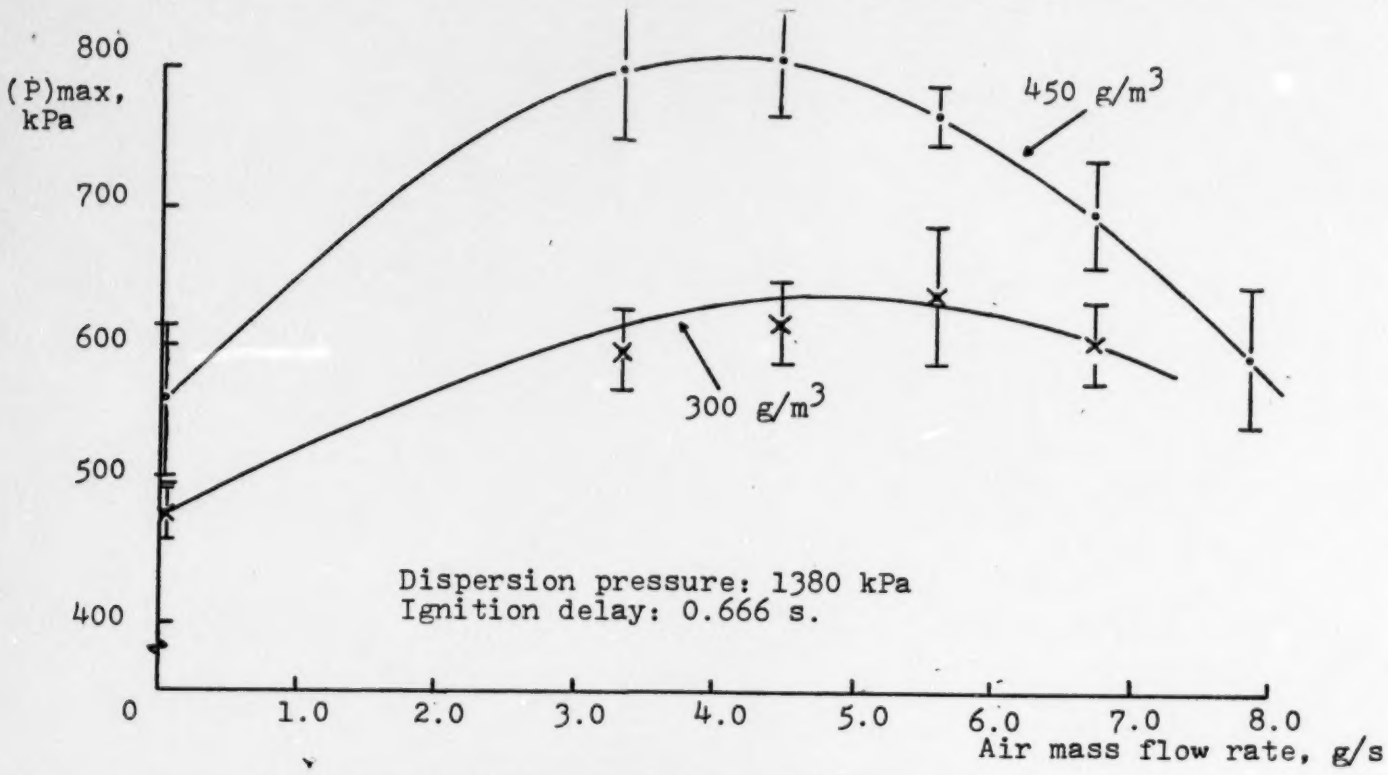

Figure 5a - MAXIMUM OVERPRESSURE VS. TURBULENCE LEVEL

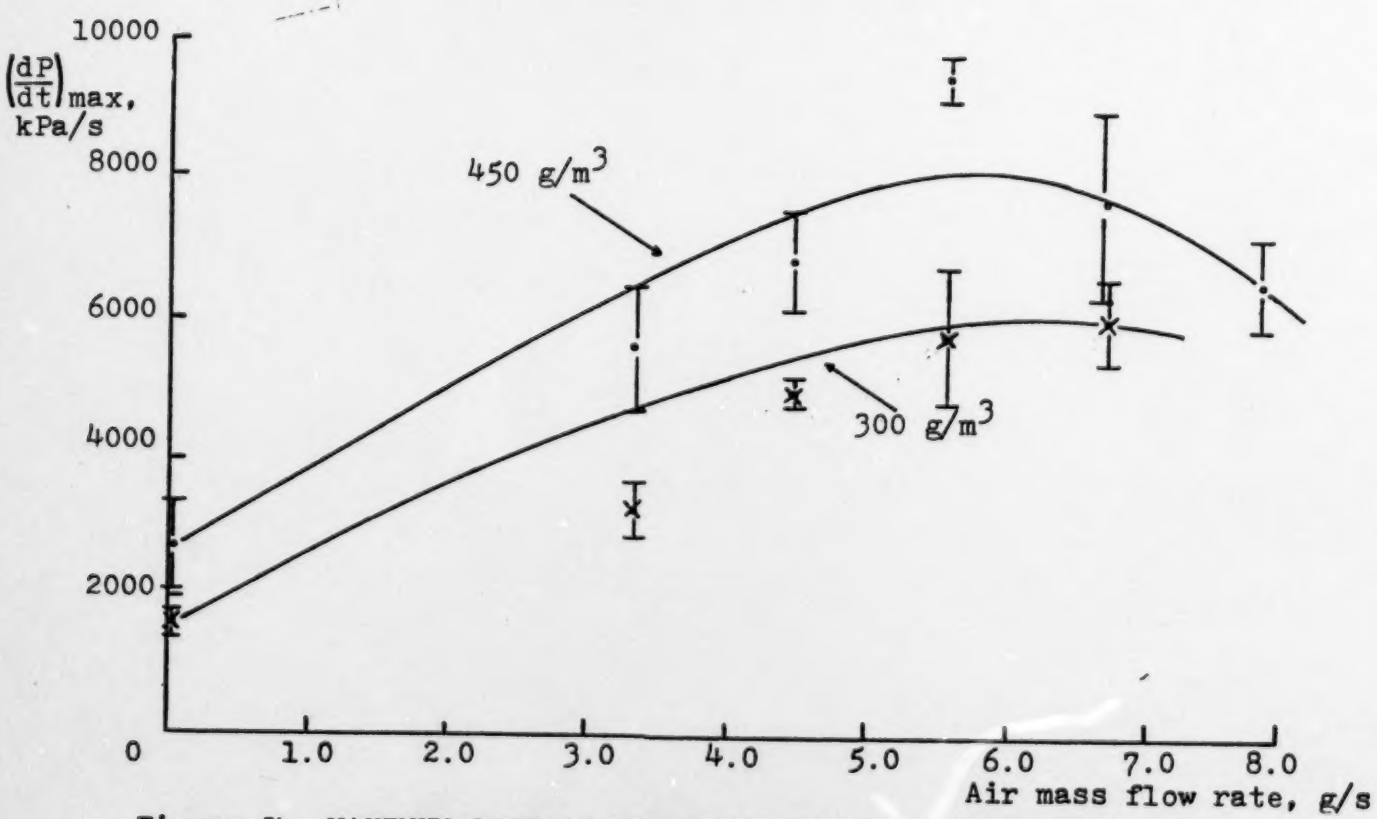

Figure 5b - MAXIMUM RATE OF PRESSURE RISE VS. TURBULENCE LEVEL

FIGURE 6- EXPERIMENTAL SETUP FOR METHANE-AIR EXPLOSIONS

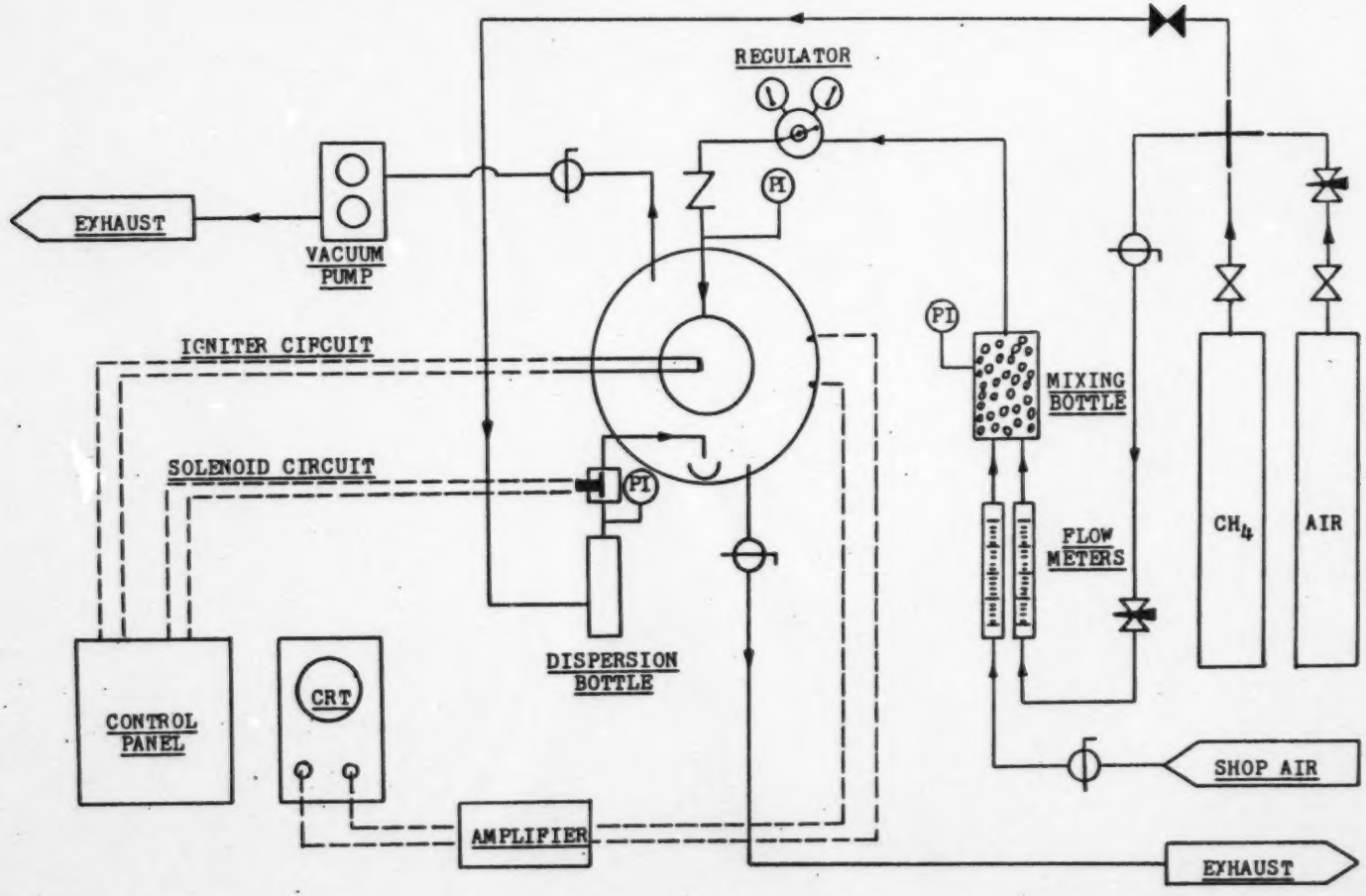

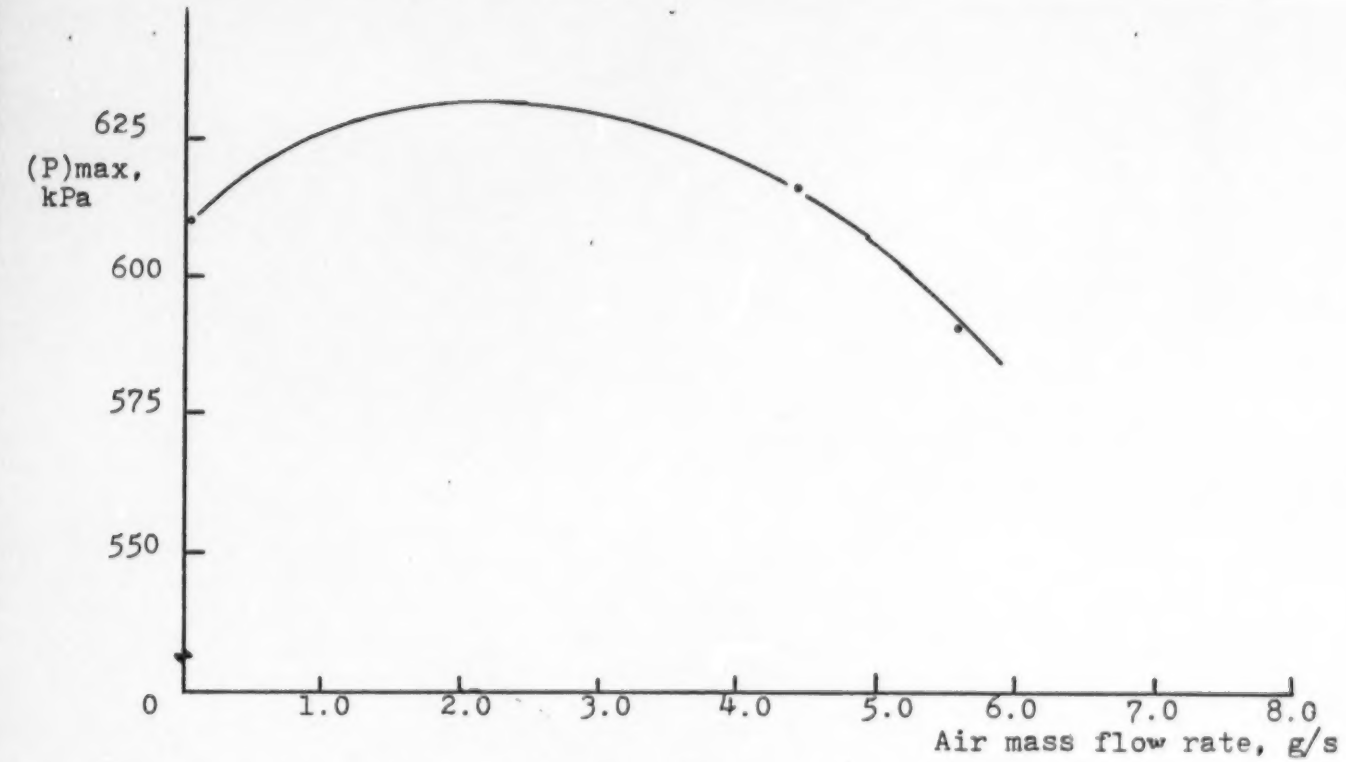

Figure 7 - METHANE-AIR EXPLOSIONS. MAXIMUM OVERPRESSURE VS. TURBULENCE LEVEL

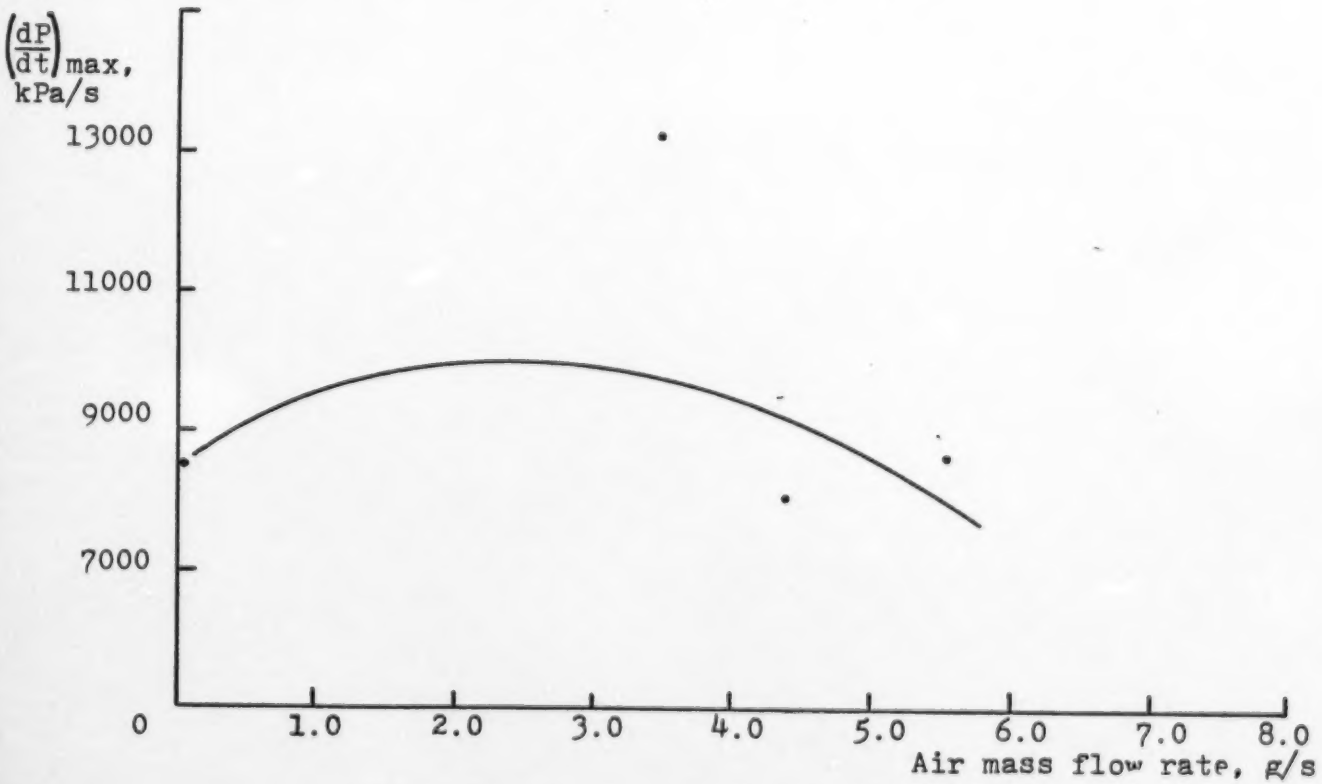

Figure 8 - METHANE-AIR EXPLOSIONS. MAXIMUM RATE OF PRESSURE RISE VS. TURBULENCE LEVEL

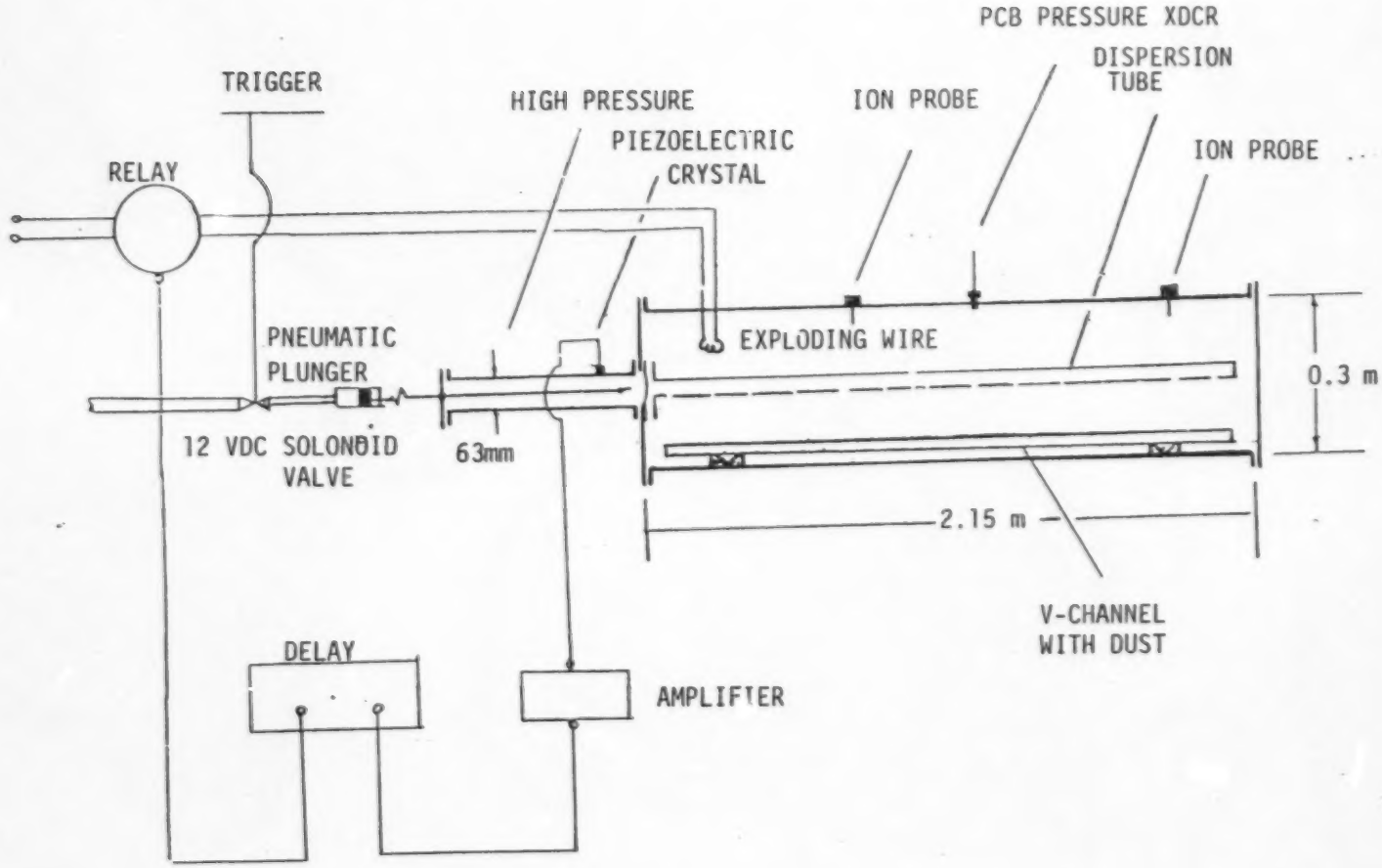

SCHEMATIC OF APPARATUS

FIG. 9(a)

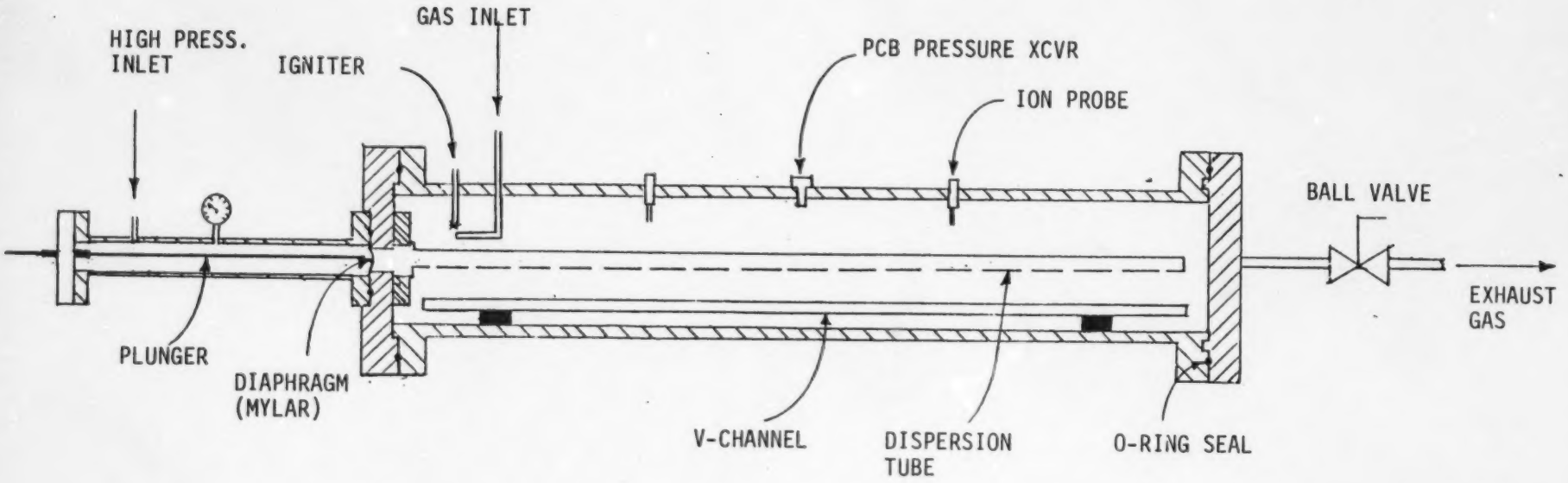
HIGH PRESS.
INLET
IGNITER
GAS INLET
PCB PRESSURE XCVR
ION PROBE
BALL VALVE
EXHAUST
GAS
PLUNGER
DIAPHRAGM
(MYLAR)
V-CHANNEL
DISPERSION
TUBE
O-RING SEAL

FIG. 9(b)

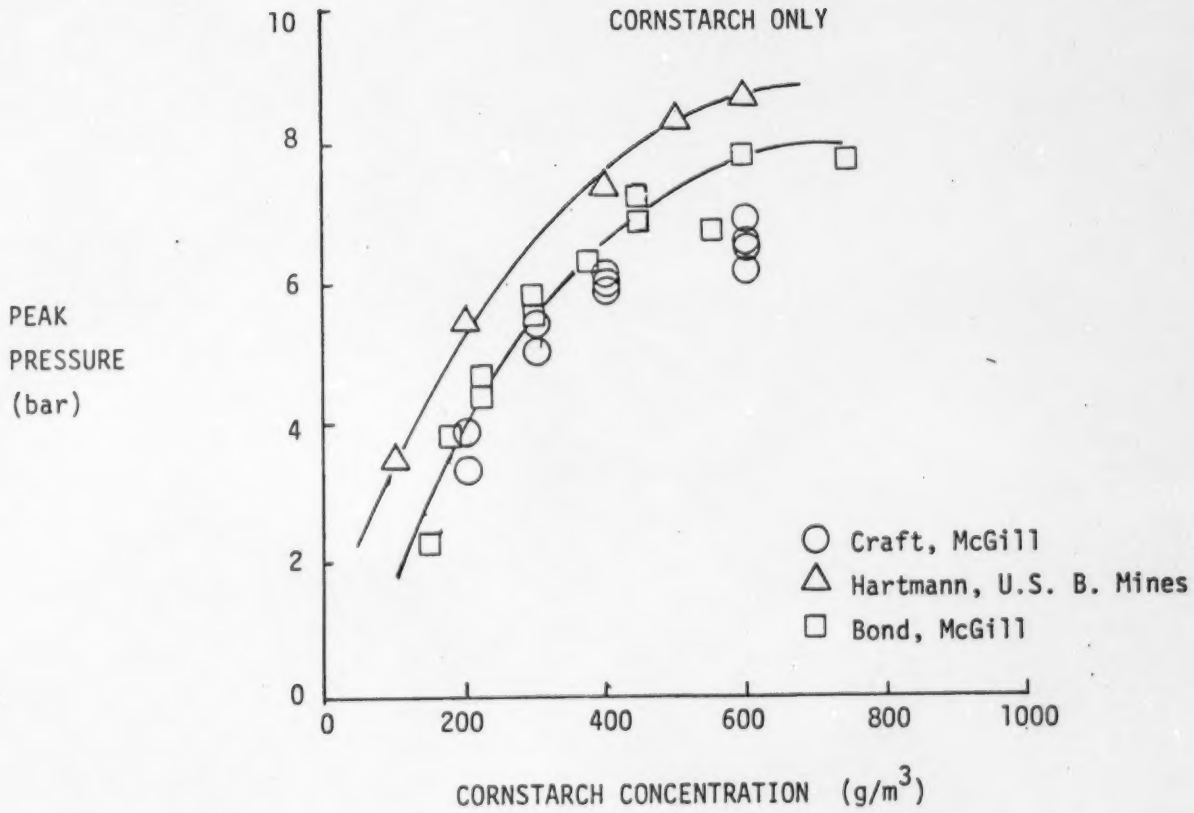
CORNSTARCH ONLY
PEAK
PRESSURE
(bar)
10
8
6
4
2
0
0
200
400
600
800
1000
CORNSTARCH CONCENTRATION (g/m3)
Craft, McGill
Hartmann, U.S. B. Mines
Bond, McGill

FIG. 10

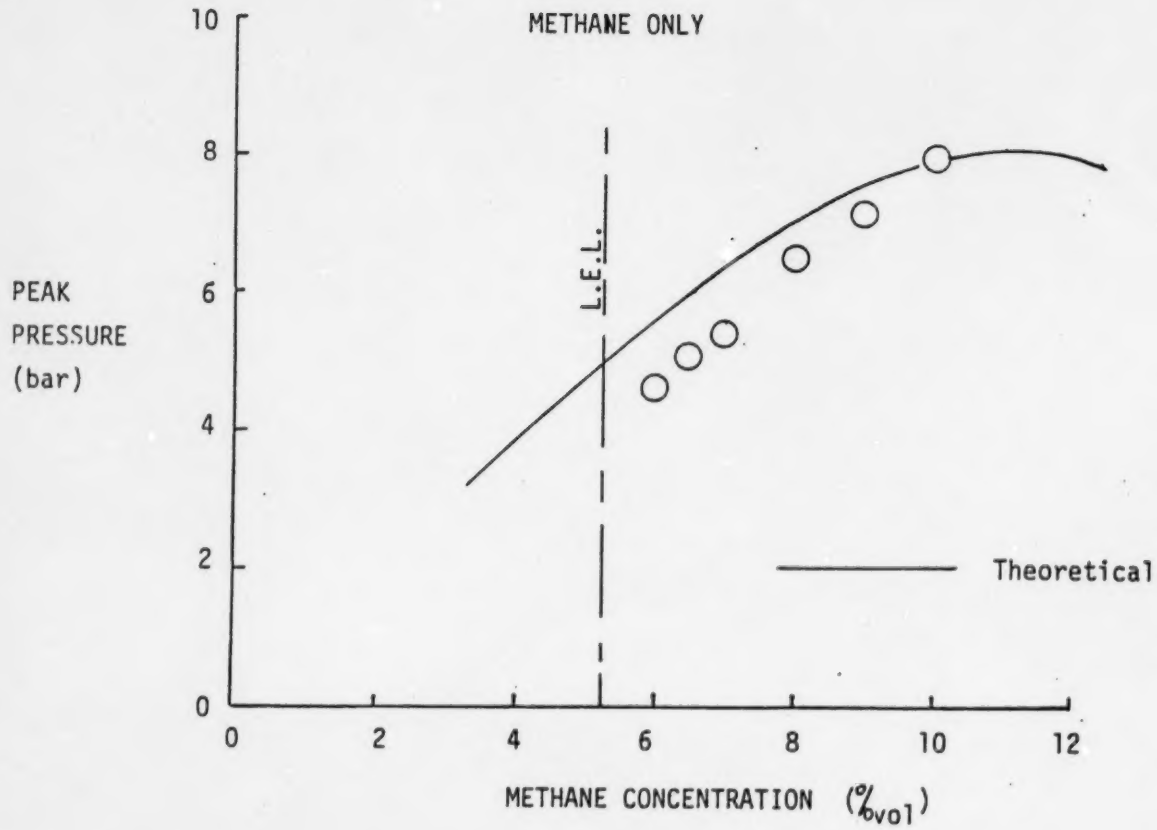
METHANE ONLY
PEAK
PRESSURE
(bar)
10
8
6
4
2
0
L.E.L.
Theoretical
0
2
4
6
8
10
12
METHANE CONCENTRATION (%vol)

FIG. 11

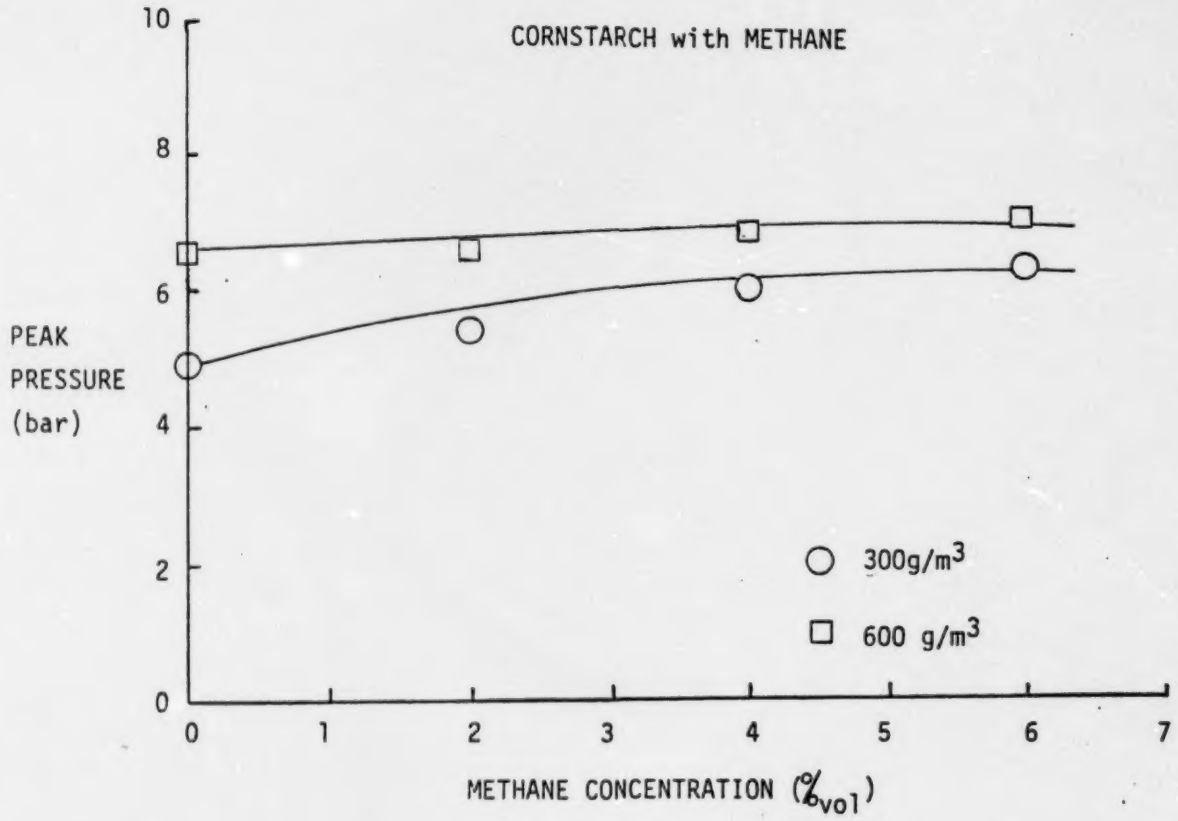
CORNSTARCH with METHANE
PEAK
PRESSURE
(bar)
10
8
6
4
2
0
0
1
2
3
4
5
6
7
300g/m3
600 g/m3
METHANE CONCENTRATION (%vol)

FIG. 12

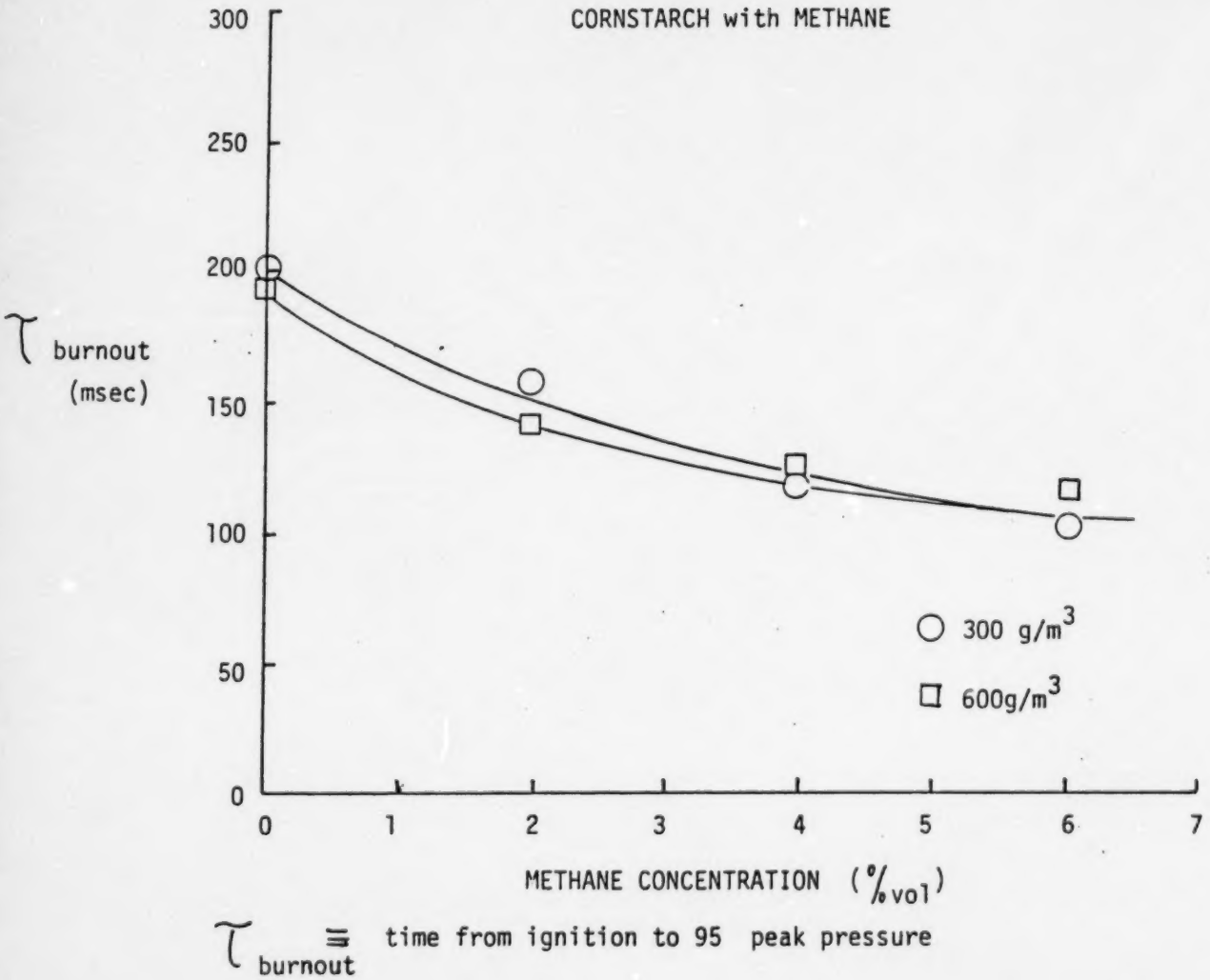

$\tau_{burnout} \equiv$ time from ignition to 95 peak pressure

FIG. 13

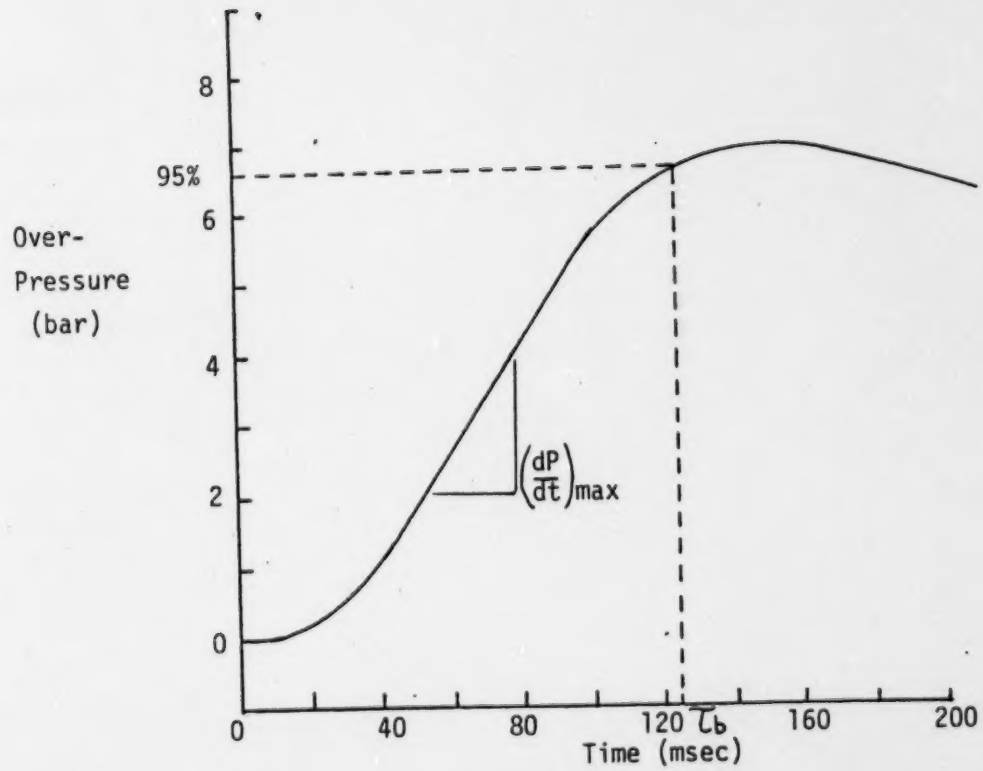

TYPICAL PRESSURE - TIME HISTORY

FIG. 14

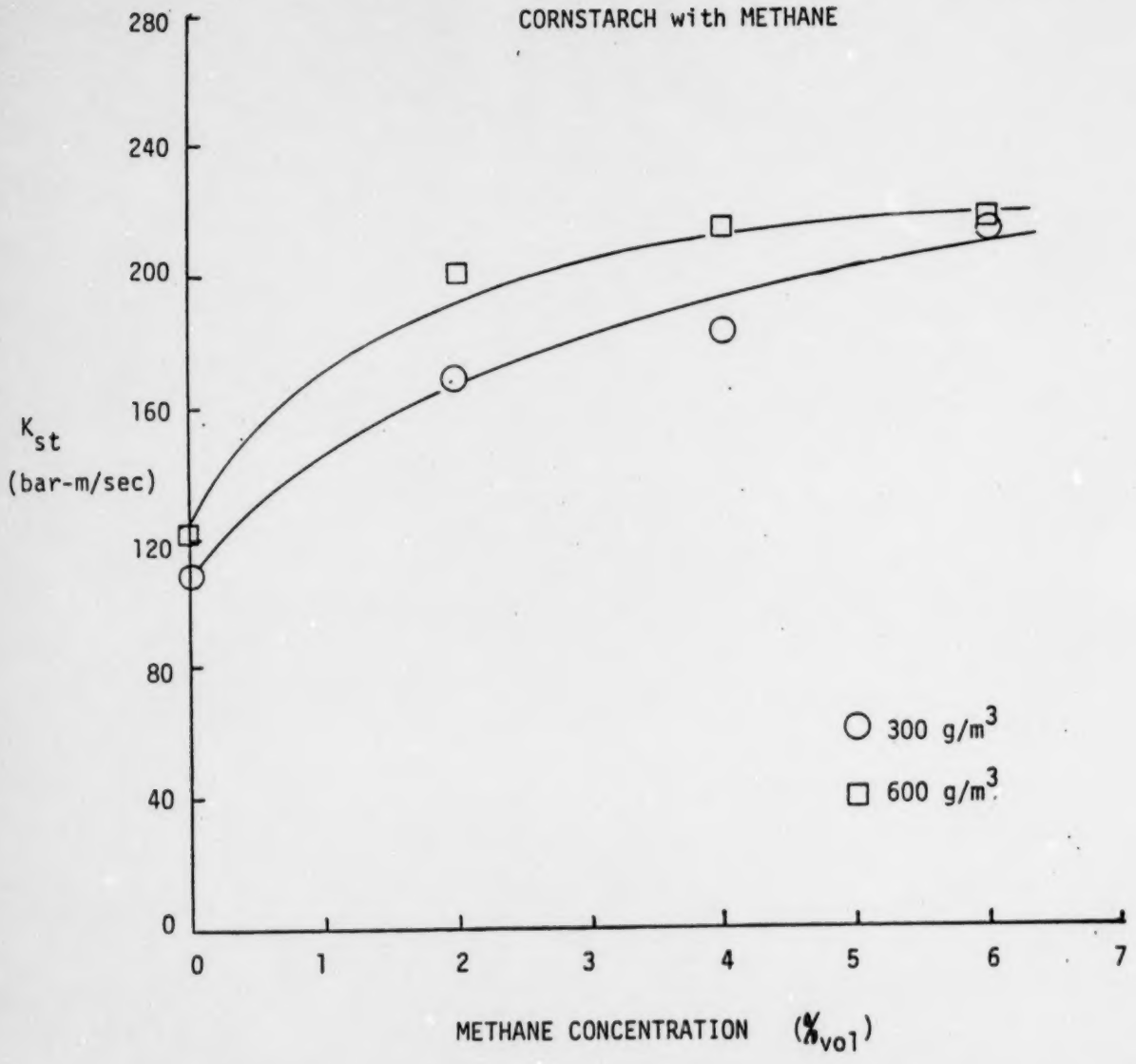

$$K_{st} = \left(\frac{dP}{dt}\right)_{max} * L_c$$

FIG. 15

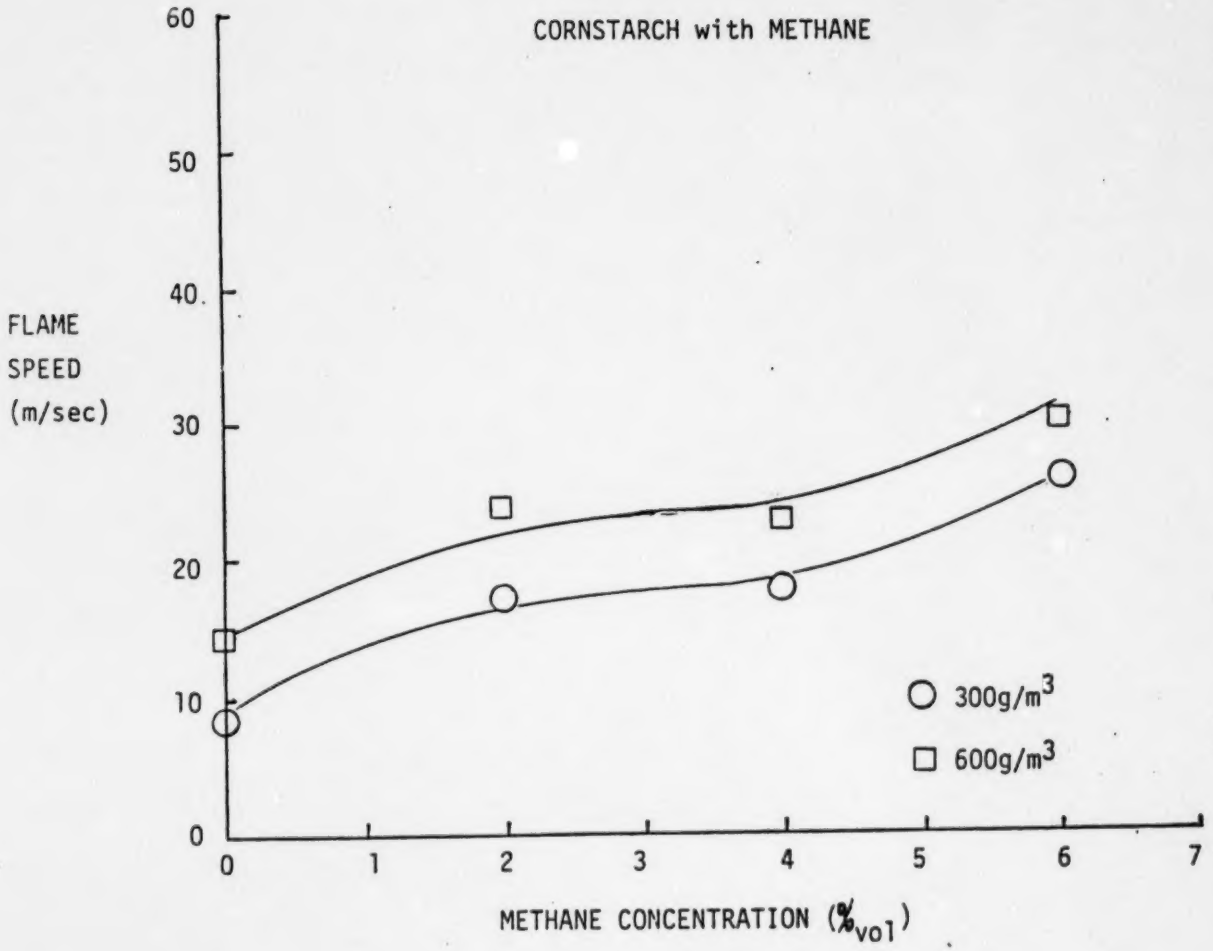
CORNSTARCH with METHANE
FLAME SPEED (m/sec)
60
50
40
30
20
10
0
0
1
2
3
4
5
6
7
300g/m3
600g/m3
METHANE CONCENTRATION (%vol)

FIG. 16

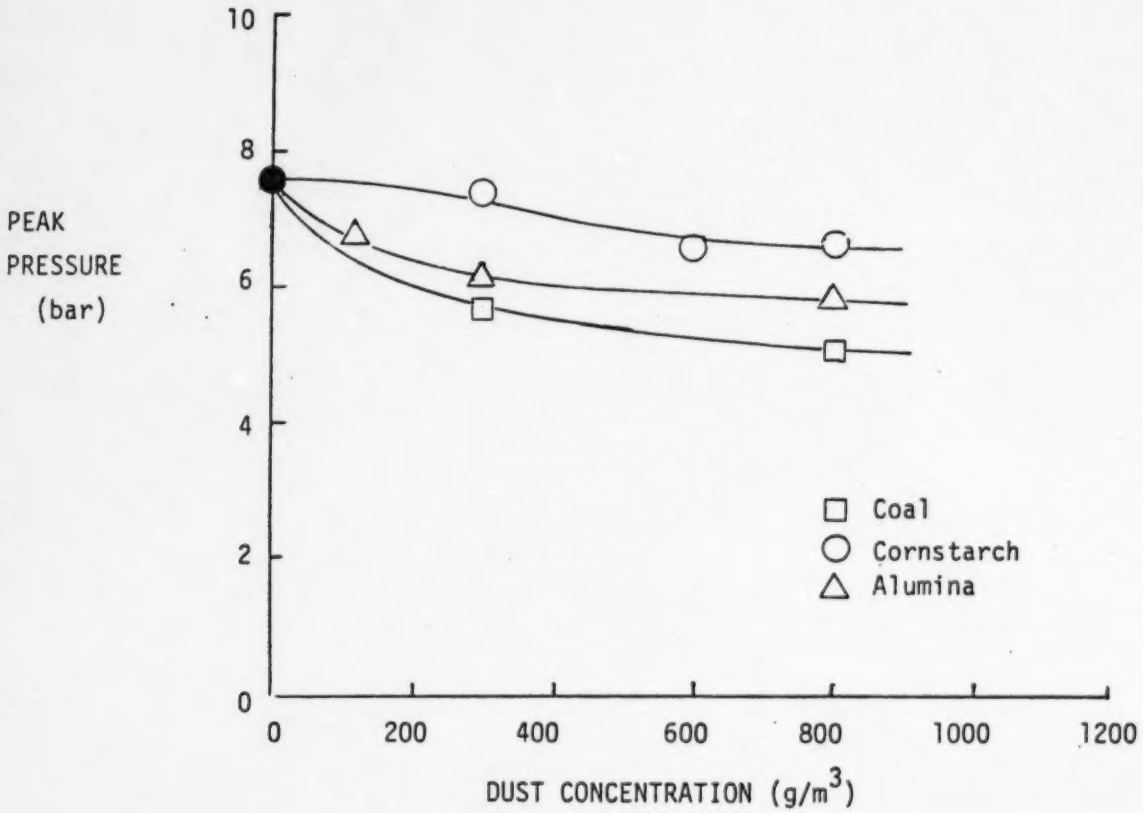
PEAK
PRESSURE
(bar)
10
8
6
4
2
0
0
200
400
600
800
1000
1200
DUST CONCENTRATION (g/m3)
Coal
Cornstarch
Alumina

FIG. 17

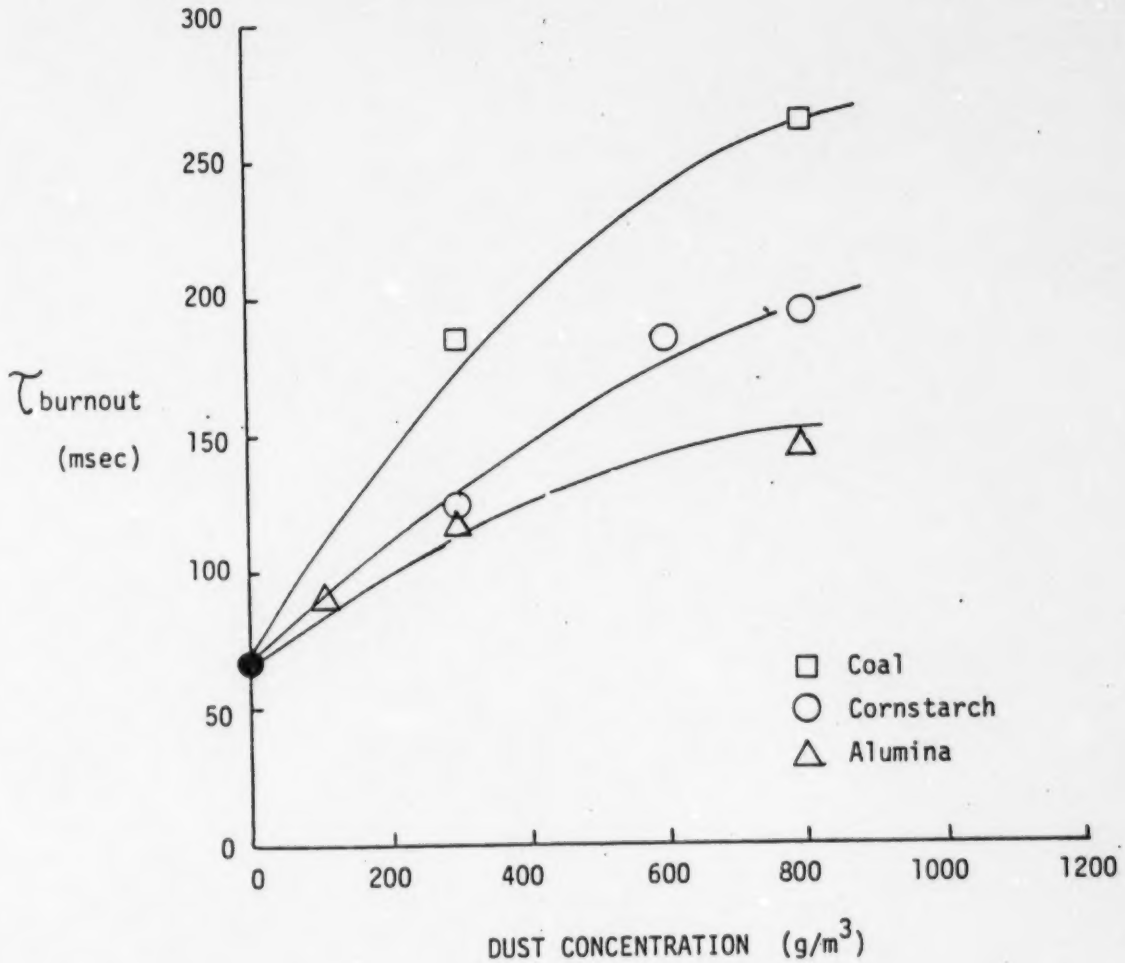

$\tau_{burnout}$ ≡ Time from ignition to 95% peak pressure

FIG. 18

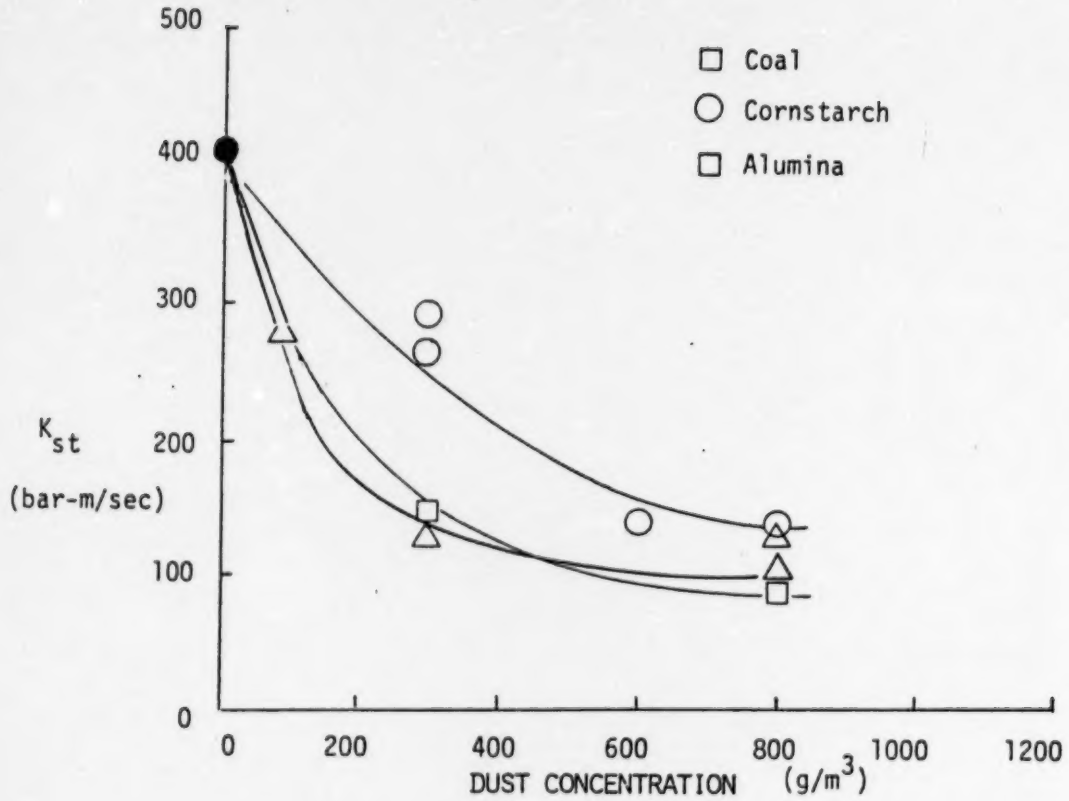

$$K_{st} = \left(\frac{dP}{dt}\right)_{max}^{*} L_c$$

FIG. 19

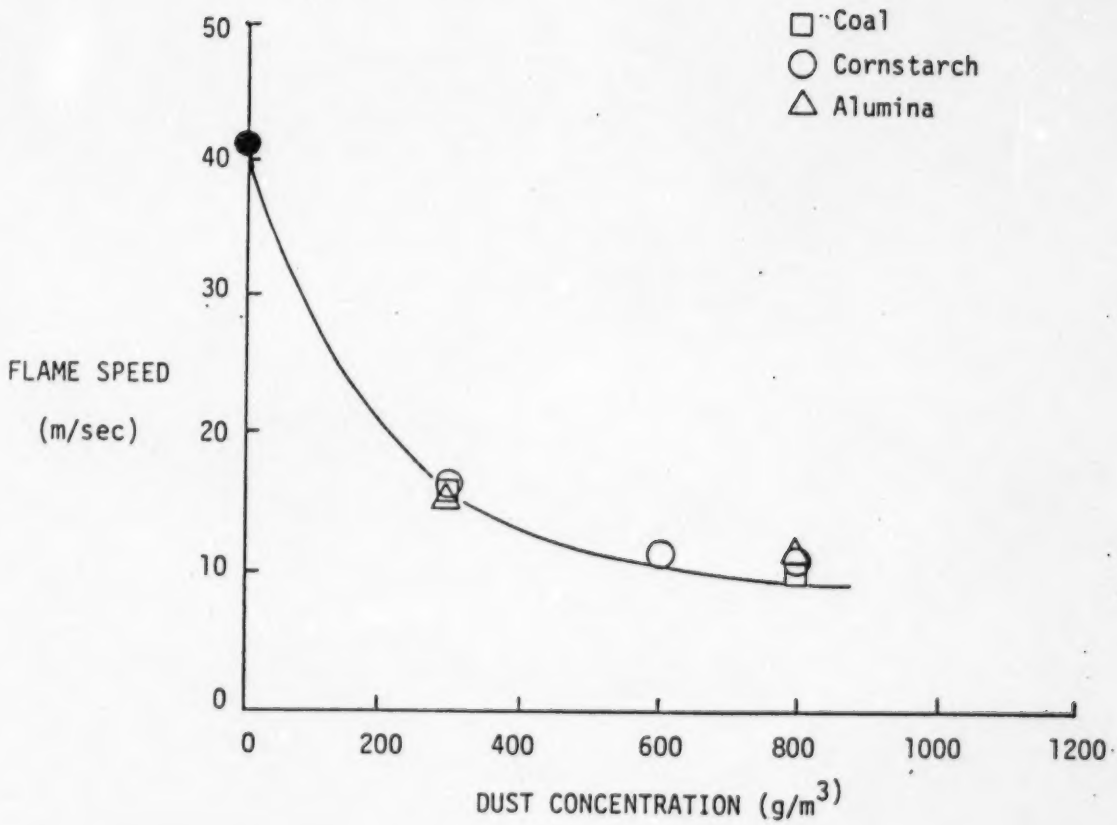
Coal
Cornstarch
Alumina
50
40
30
20
10
0
FLAME SPEED
(m/sec)
0
200
400
600
800
1000
1200
DUST CONCENTRATION (g/m3)

FIG. 20

Figure 21- EFFECT OF FERRIC OXYDE ADDITION ON EXPLOSION CHARACTERISTICS

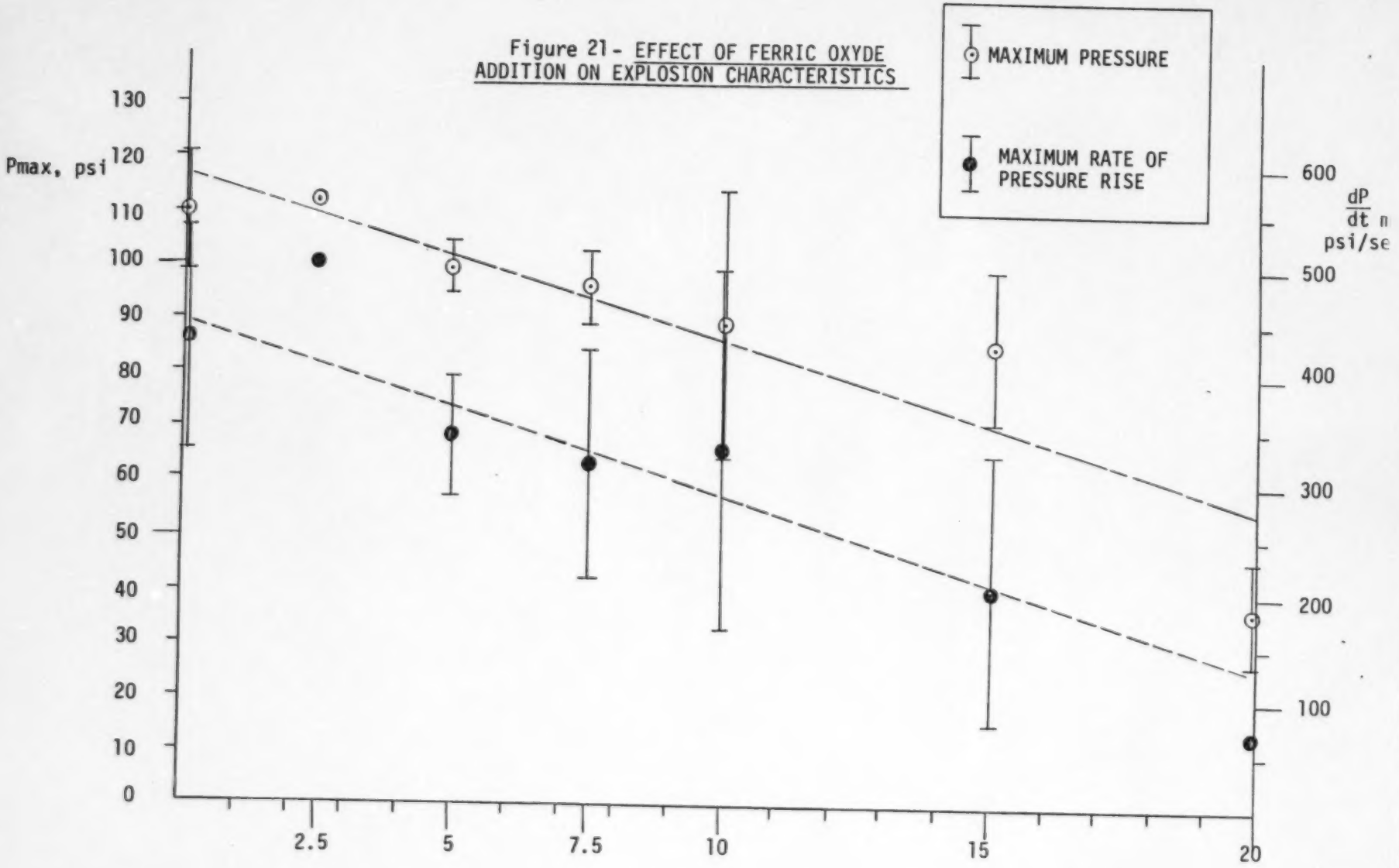

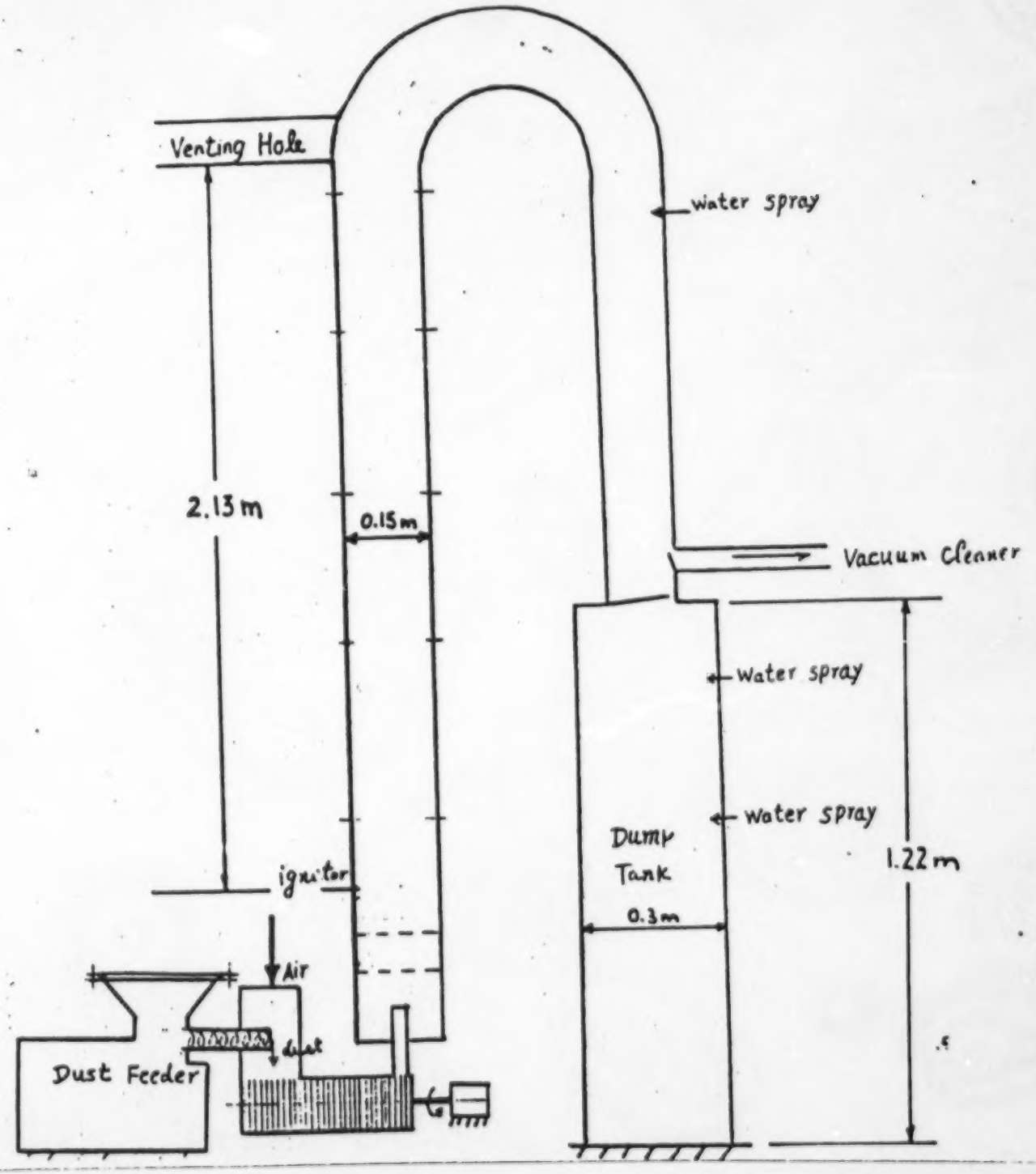

FIG. 22 - Dust Flame Acceleration apparatus - I

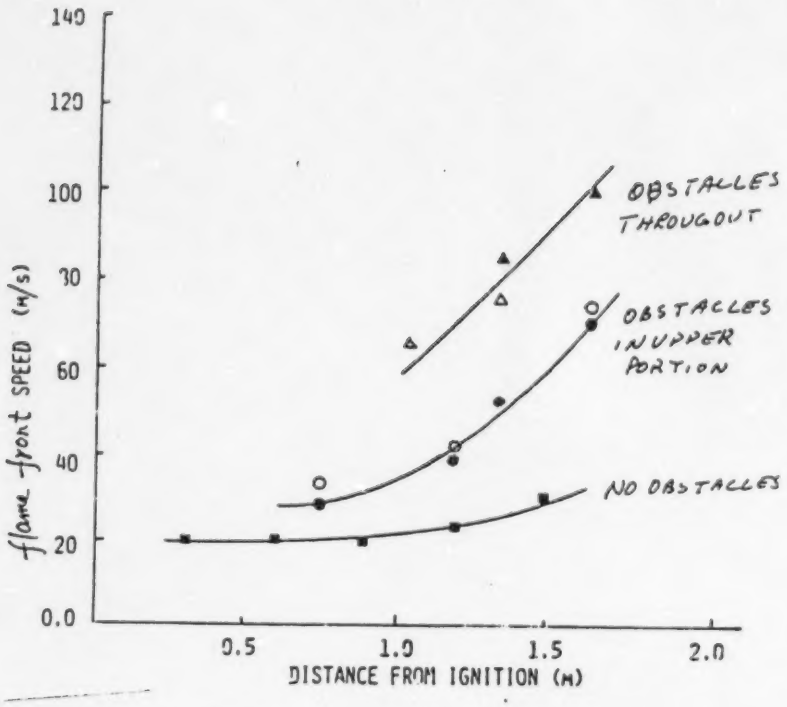

FIG. 23a - Acceleration of the Dust Flame-Front

	NO OBSTACLES	OBSTACLES IN UPPER HALF ONLY	OBSTACLES THROUGHOUT
VMAX AT THE TOP OF THE TUBE	30 M/S	75 M/S	100 M/S
$\left(\frac{dP}{dT}\right)_{MAX}$	47 $\frac{BAR}{SEC}$	89 $\frac{BAR}{SEC}$	127 $\frac{BAR}{SEC}$

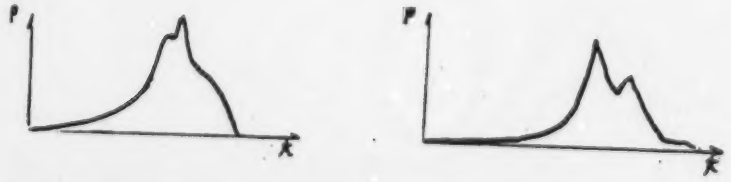

FIG. 23b - Summary of Pressure Records

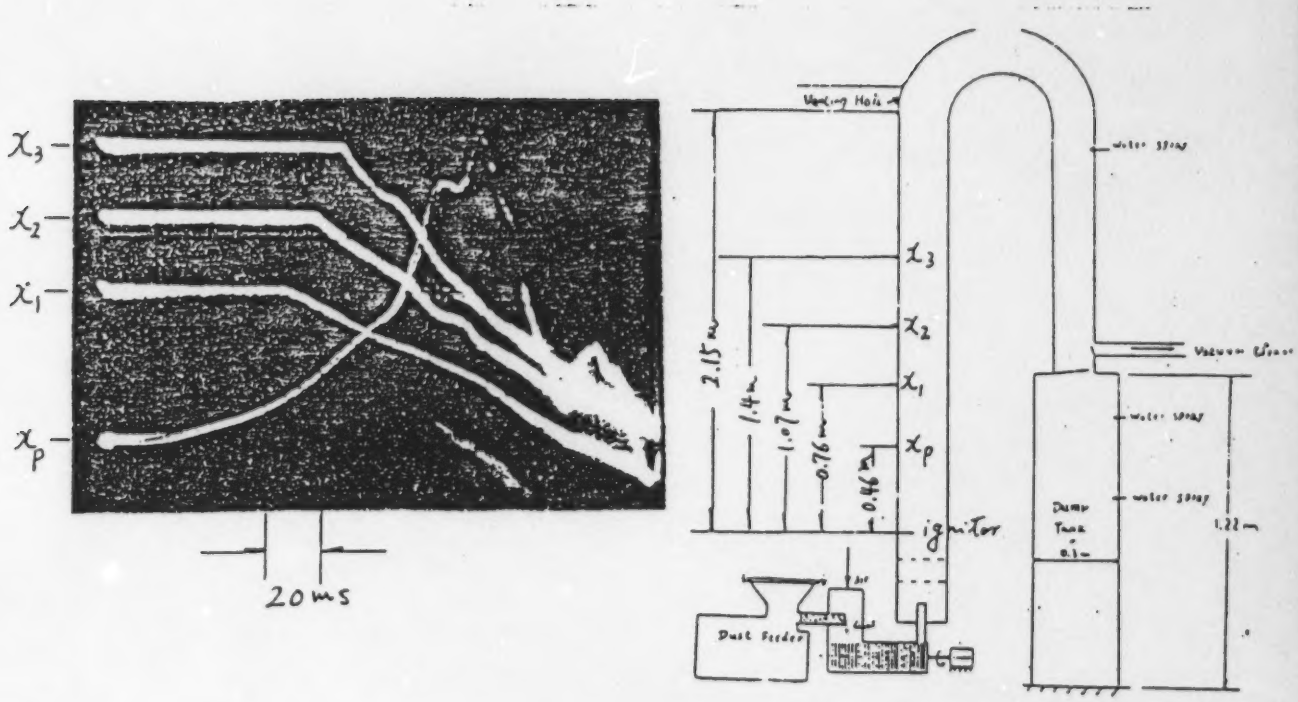

FIG. 24 - Temperature Measurement of Dust Flame

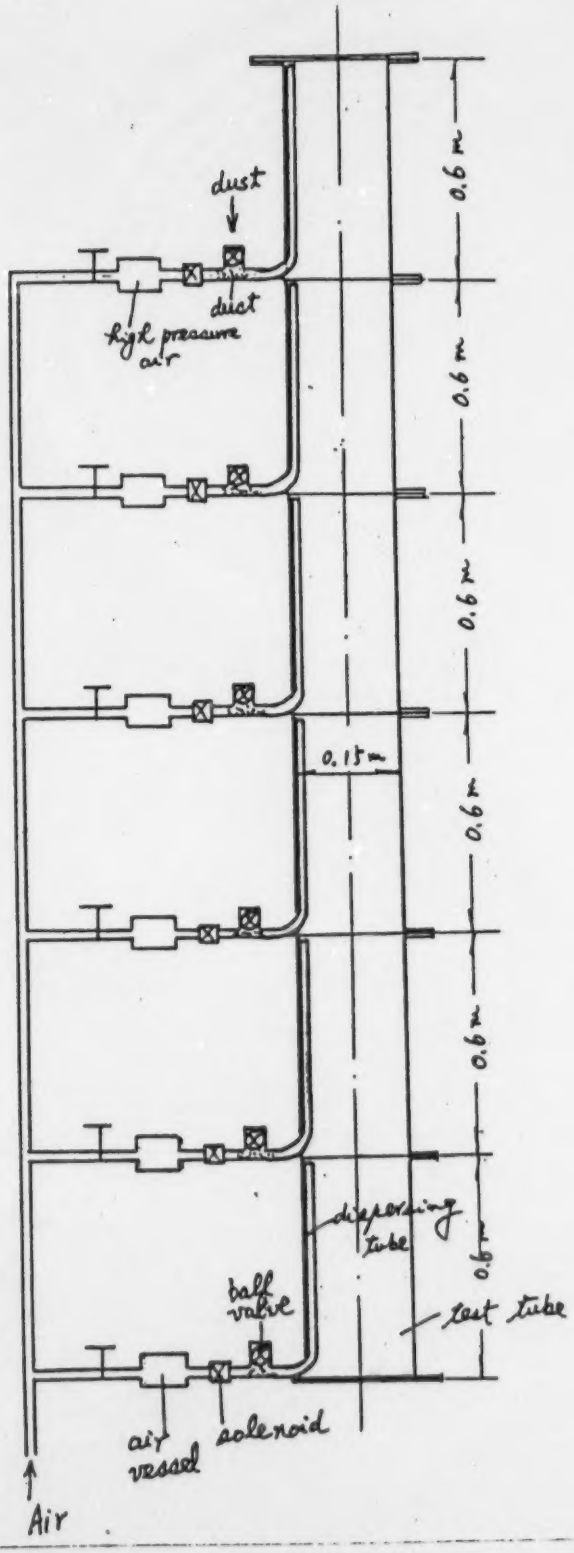

FIG. 25 - Dust Flame Acceleration Apparatus - II

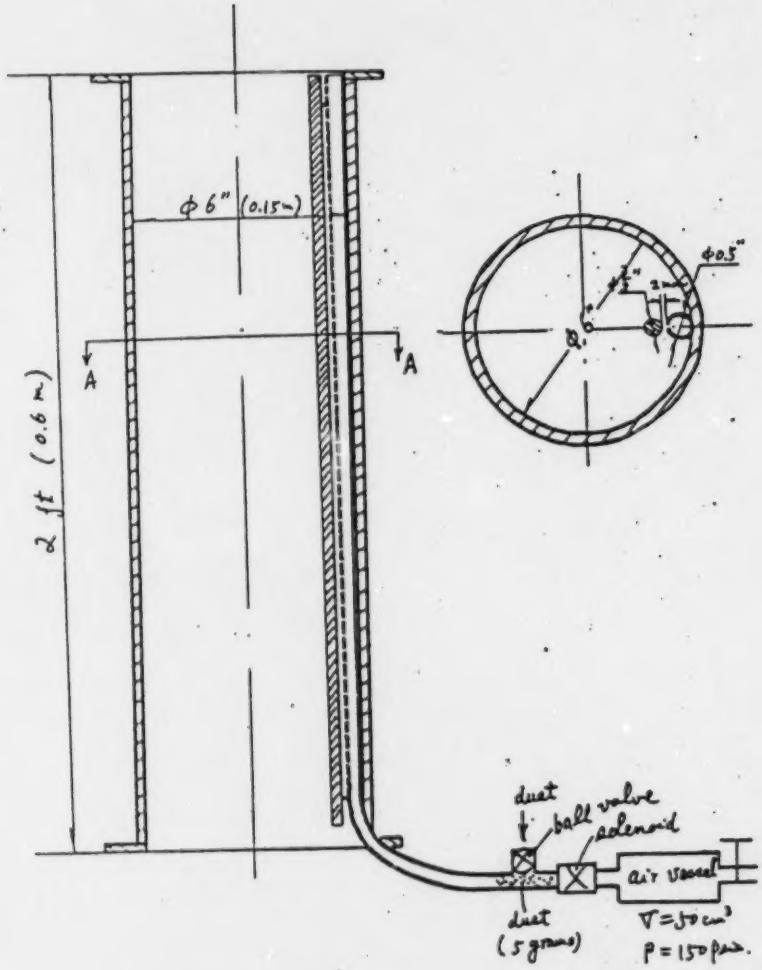

FIG. 26 - One Segment of Apparatus - II

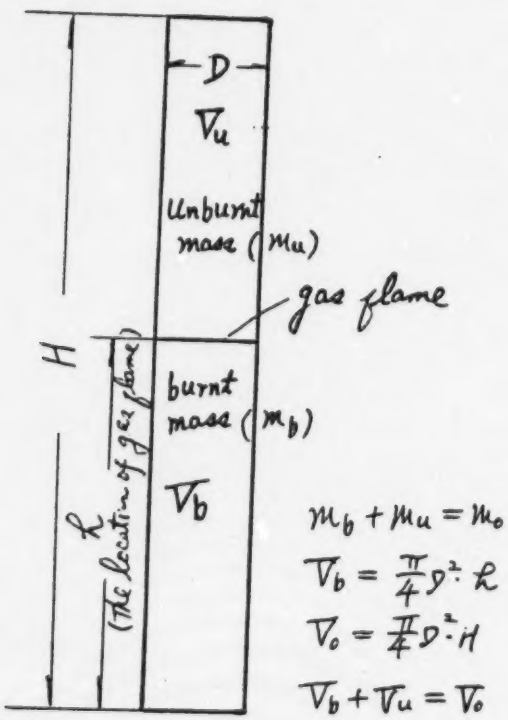

FIG. 27 - Diagram of Gas Flame

APPENDIX A

Cylindrical Bomb for Dust Combustion Studies

A cylindrical bomb of 1.0 m height and 0.5 m diameter was recently designed and built at McGill. The appratus, depicted in Figs. A1 and A2 is equipped with many circular ports for instrumentation and piping. A system of dust dispersion similar to that used in the 333 liter sphere was implemented in the cylindrical bomb.

This apparatus will be used in conjunction with the other pieces of equipment described to study scaling effects. By comparing pressure records from the 333 liter sphere, the circular tube and the cylindrical bomb, for instance, the validity of Barthnecht's cubic law of dust combustion[2] may be assessed. The effect of turbulence in a different geometry and using different means of inducing turbulence can be studied in this apparatus. This bomb can also be interfaced with a 70 cm circular tube to study transmission of a dust deflagration from a tube into essentially open space.

TEST APPARATUS
(V = 0.180 m^3)

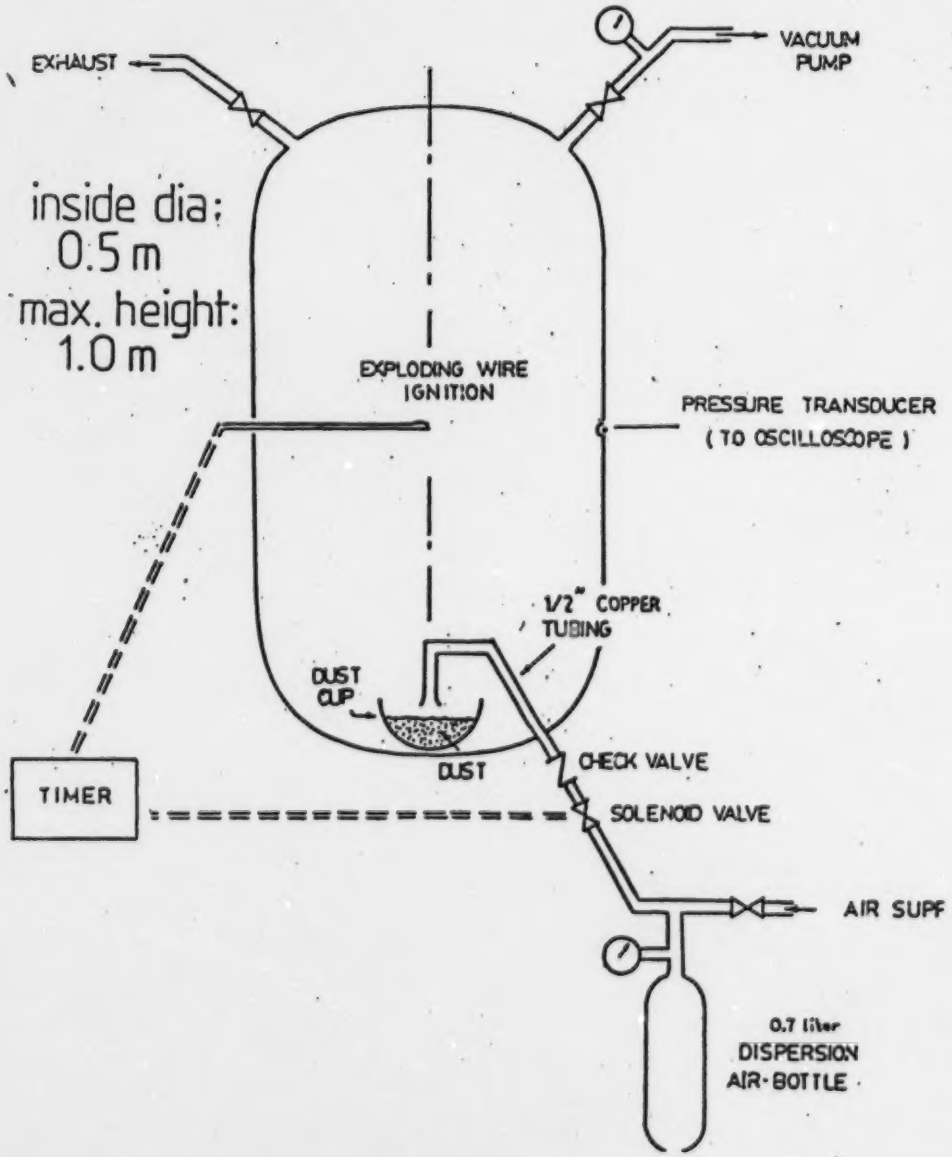

FIG. A1

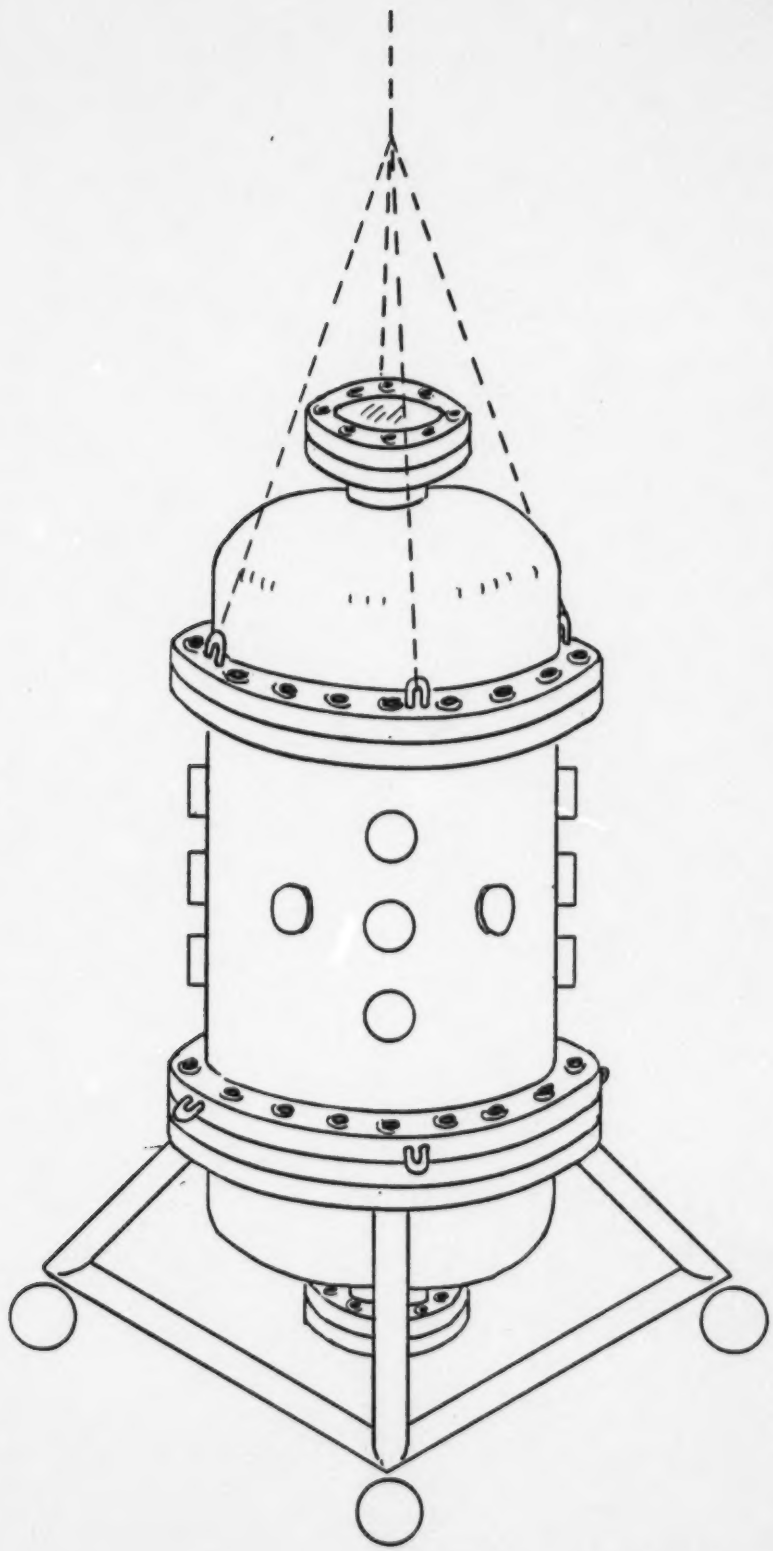

FIG. A2

ISOMETRIC VIEW OF APPARATUS	
DWG NO: 15	DATE: NOV 1, 1983
SCALE: 1:10 (INCHES)	DWN BY: M. FRESKO

APPENDIX B

Some Testing and Measurements for Dust Dispersion

Systematic testing and measuring is the proper way to study the uniformity of dust dispersion system designed as Fig. 1 because the mechanism of dispersing process is too complex to try any analysis.

An optical measurement system shown in Fig. 2 and a 22" x 13" x 30" box for testing the dust dispersion device shown in Fig. 3 has been set up to study the uniformity of the dust dispersion along a segment of the test tube described earlier. By converting the light transmission through the 13" box to an electronic signal via a 929 photo-multiplier tube a quantitative measurement of the dust concentration can be made as illustrated in Fig. 2. This measurement is made at three distances in the horizontal direction from the dispersion tube and at two different heights, one near the top, the other near the bottom, in order to analyze the spacial and temporal uniformity of the dispersion. Figures 4 and 5 show some typical results. The zero line, located at the top of the figure, corresponds to 100% transmission. The line at the bottom corresponds to zero transmission of light.

Experimental results show:

1. The uniformity of dust concentration between the top and bottom section depends on the arrangement of the tube diameter and the number of small dispersing holes. The arrangement of small dispersion holes is shown by Fig. 7(1). In Fig. 6, the dispersion holes are kept the same diameter (41 mm) and distributed uniformly. It is obvious that the dispersion generated by the arrangement shown in Fig. 7(1) is superior to that produced by the arrangement shown in Fig. 7(2).

2. The uniformity of dust suspended over a period of 1 sec depends on the exit velocity of jet emerging from the small dispersion holes. The jet velocity mainly depends on the air pressure in the vessel before dispersion. From tests we know that dispersing 5 grams (cornstarch + 2% Cab-o-sil) from the bottom end of an 0.5" diameter dispersion tube 2 ft long, a 50 cm^3 reservoir must be pressurized to 150 psig. In this case, the exit velocity of jet is almost 9 m/sec which can be estimated from the curves of optical transmission measurements. Figure 8 shows the velocity of the jet in the bottom section for different distances from the dispersion tube.

Figure 4 shows that when the velocity of jet is high (9 m/sec) most of the dust has been dispersed into the test box within the first 0.2 second. If the diameter of the test tube is small (approx. 6"), the dusty jet will impact against the wall opposite the jet. After the inelastic collision with the wall, the dust will fall down along the wall. In such a case the concentration gradients in space and time will be severe.

Figure 5 shows that when the velocity of jet decreases to 1.5 m/sec, the uniformity of dust suspension within 0.5 $\sim$ 1 sec duration is improved.

3. A circular rod with diameter 3/8" and square bar 1/4" x 1/4" fixed in front of the dispersion tube with different gaps have been used to try to decrease the velocity of the jet. From the experimental results shown in Fig. 8, it is known that a circular rod is more efficient than a square bar in decreasing the jet velocity. When the gap between the obtacle and dispersion holes is less than 4 mm, the limit jet velocity at 6" distance from the dispersion tube is about 1.5 m/sec.

4. Figure 9 shows the difference of jet velocities between the top and bottom sections for the dispersion system designed as shown in Fig. 1.

Figure 5 shows the uniformity of dust suspension for a 1 sec duration between the top and bottom sections for the dispersion system designed as in Fig. 1. In Fig. 5, the optical transmission measurements are made by passing light through a small volume (6" x 7" x 30" as seen in Fig. 10) to consider the effect of three dimensions.

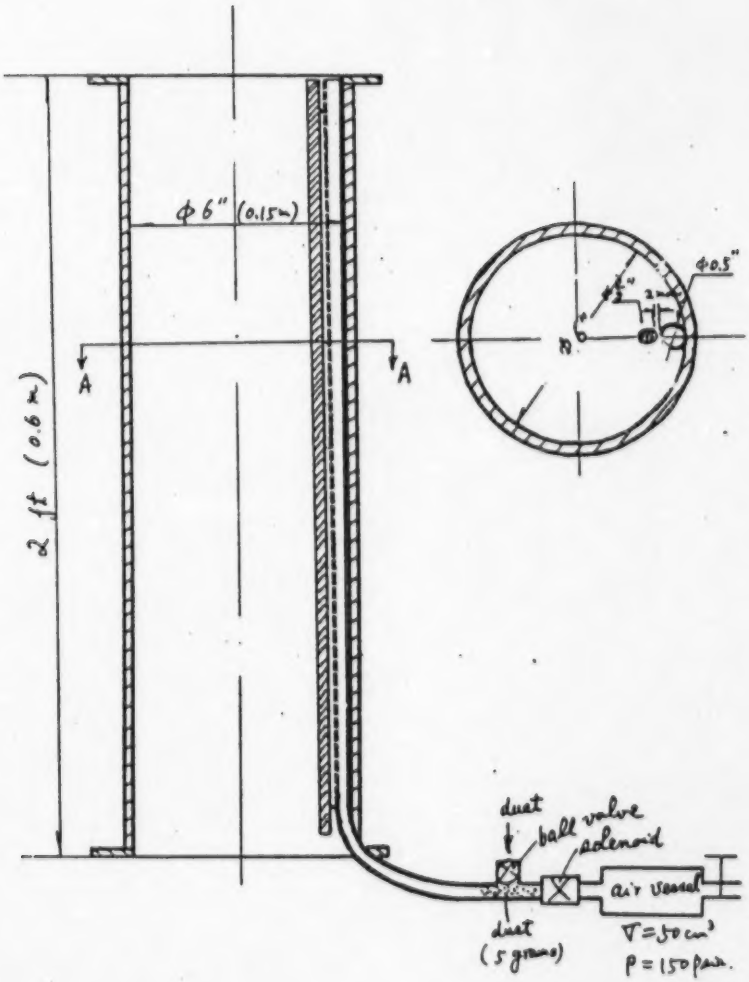

FIG. B1 - Dispersion System in a Segment

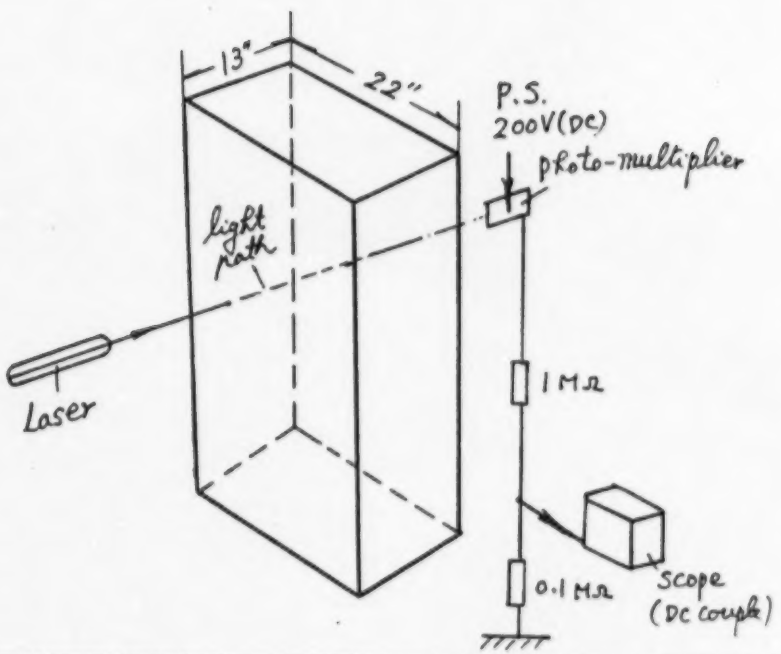

FIG. B2 - Optical Arrangement of Transmission Measurements for Dust Dispersion Experiments

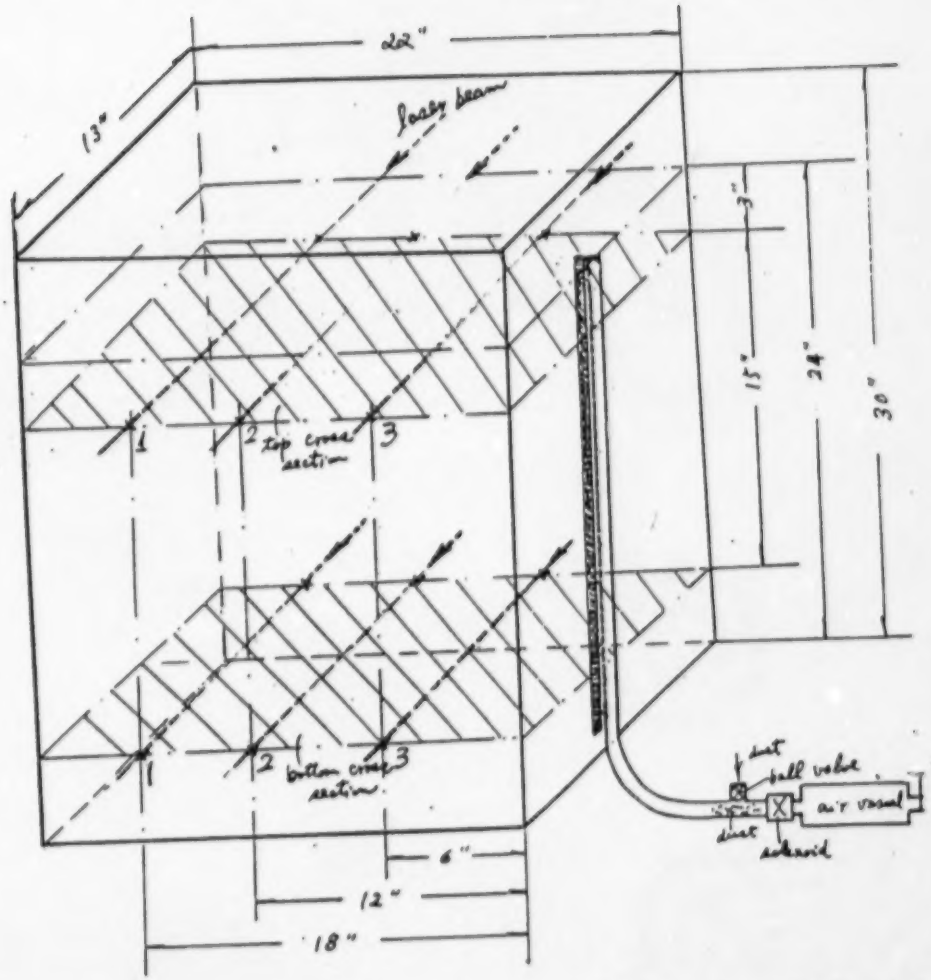

FIG. B3 - Dust Dispersion Box

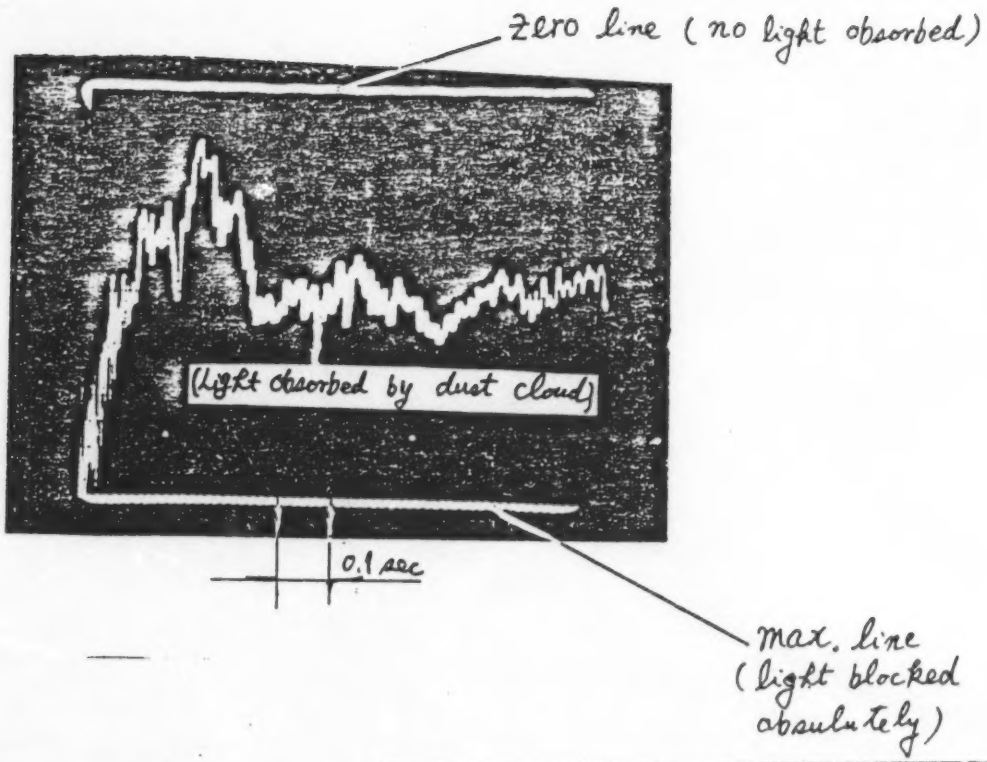

FIG. B4 - Light Transmission vs. Time(dispersion tube without bar in front)
(In Dispersion Box Bottom Section Position 3)

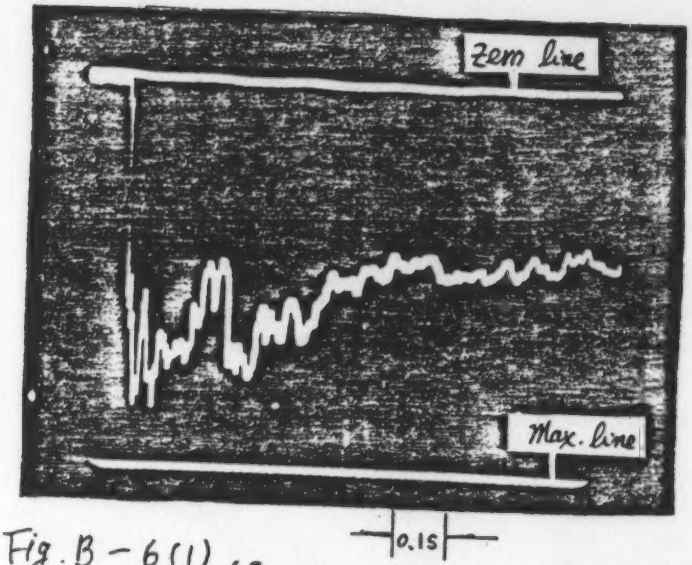

Fig. B-6(1) (In dispersion box: top section & position 3)

FIG. B6(1) - (In Dispersion box: Top Section Position 3)

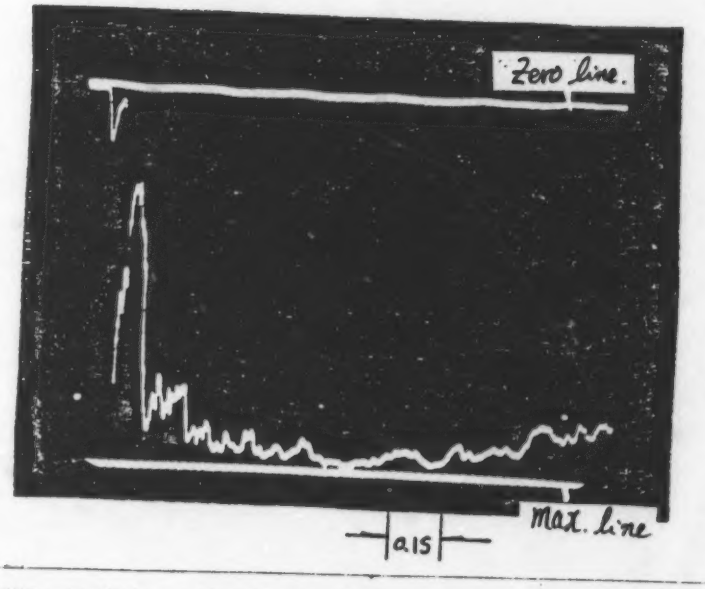

FIG. B6(2) - (In Dispersion Box: Bottom Section Position 3)
Light Transmission vs. Time (Dispersion Tube with Bar in Front)

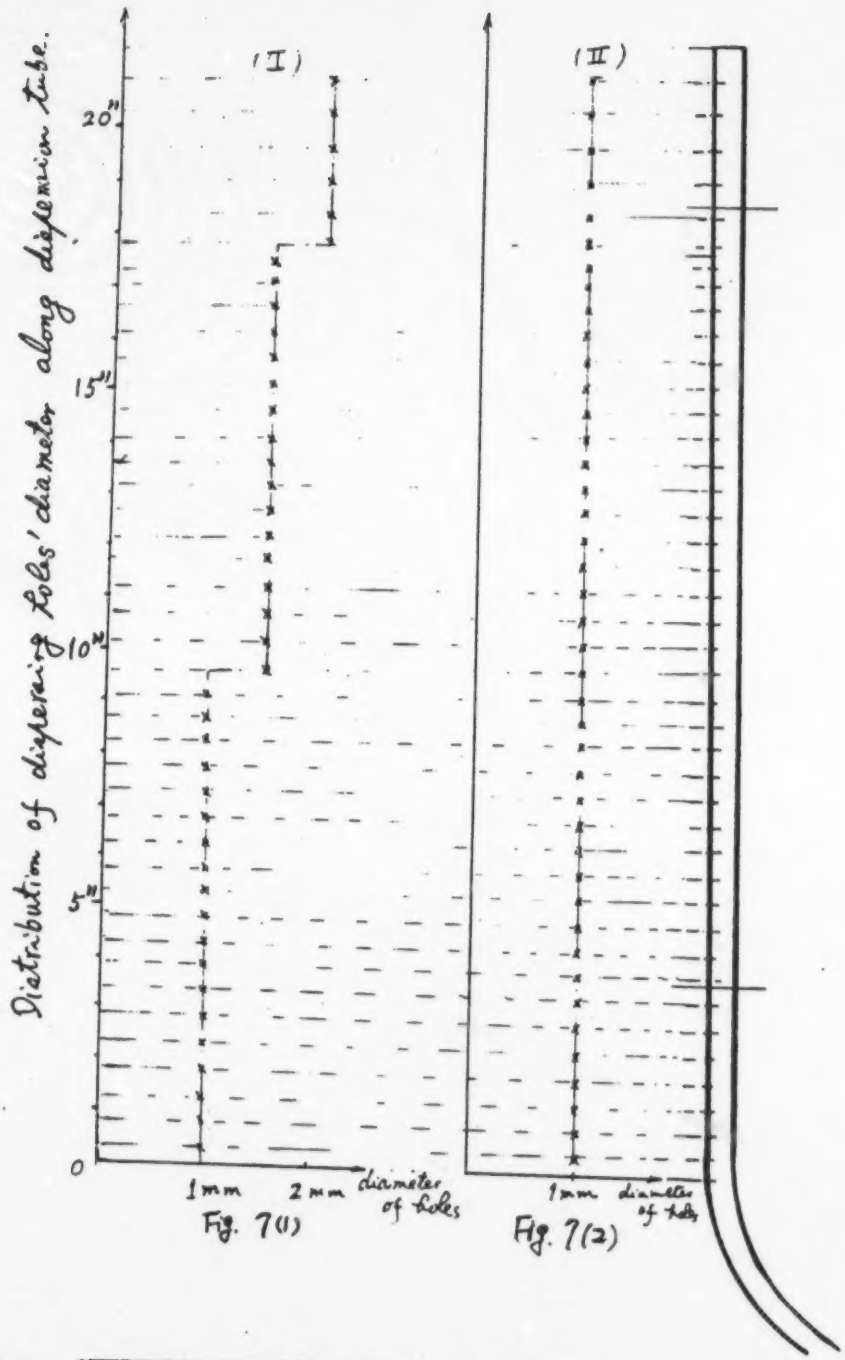

FIG. B7 - Arrangment I and II of the Distribution of Dispersing Holes Diameter

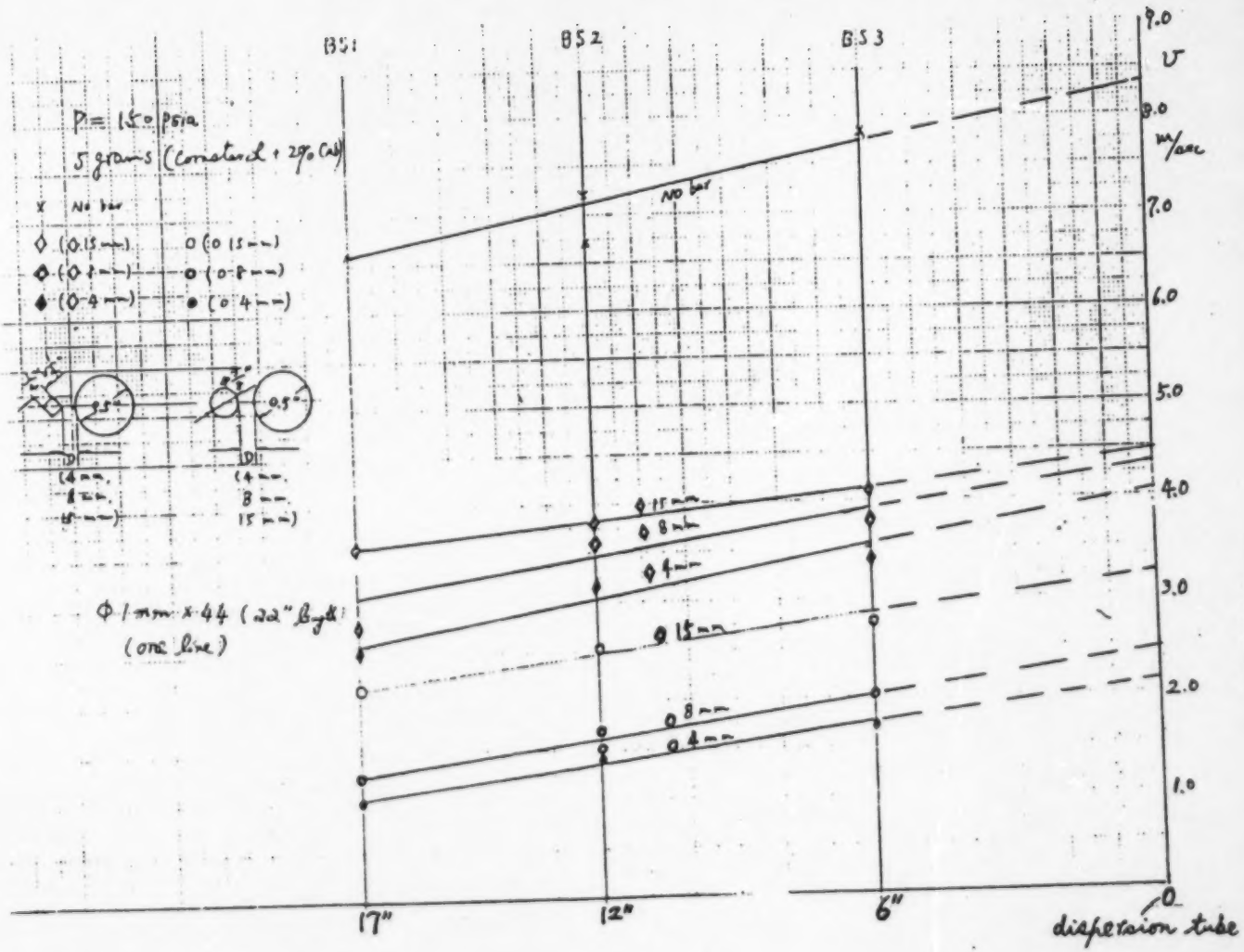

FIG. B8 - The Distribution of Jet Velocities with the distances From the Dispersion Tube (In the Bottom Section of Box)

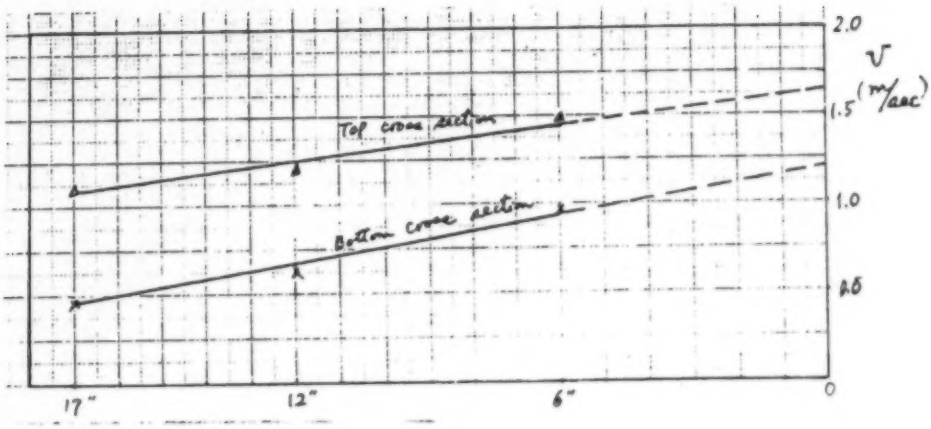

FIG. B9 - The distribution of Jet Velocities in Both of the Top and Bottom Section of Box

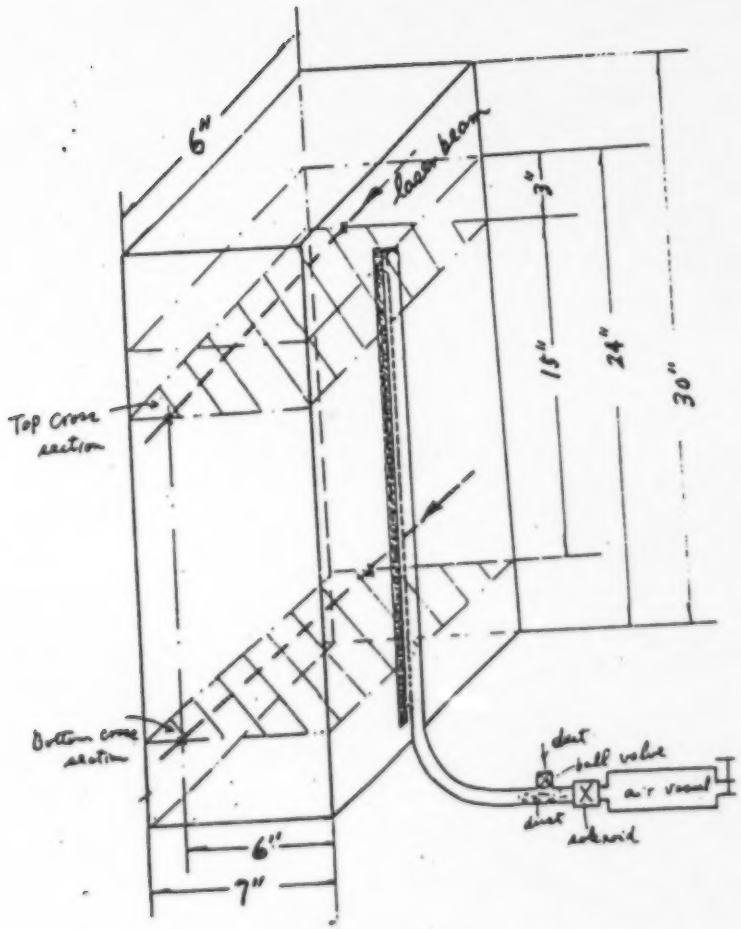

FIG. B10 - Dispersion Box with Small Volume (6" x 7" x 30")